la materia oscura

Pierre Salati – Université de Savoie & **LAPTH**

I) I nutralini di i nosci muntagni

II) I nutralini di nostro mare

III) I nutralini di i nostre isole

Cosmology and Particle Physics Beyond the Standard Models – Cargese – August 7, 2007

Direct Dark Matter Detection

Pierre Salati – Université de Savoie & **LAPTH**

1) Collision kinematics and the exclusion plot

2) Scattering cross section and nucleon content

3) The experimental endeavors and achievements

4) Future prospects

Cosmology and Particle Physics Beyond the Standard Models – Cargese – August 7, 2007

Direct Dark Matter Detection

Pierre Salati – Université de Savoie & **LAPTH**

1) Collision kinematics and the exclusion plot

2) Scattering cross section and nuclear content

3) The experimental milestones and achievements

4) Future prospects

Cosmology and Particle Physics Beyond the Standard Models – Cargese – August 7, 2007

Laboratory Frame

Elastic scattering off a nucleus at rest

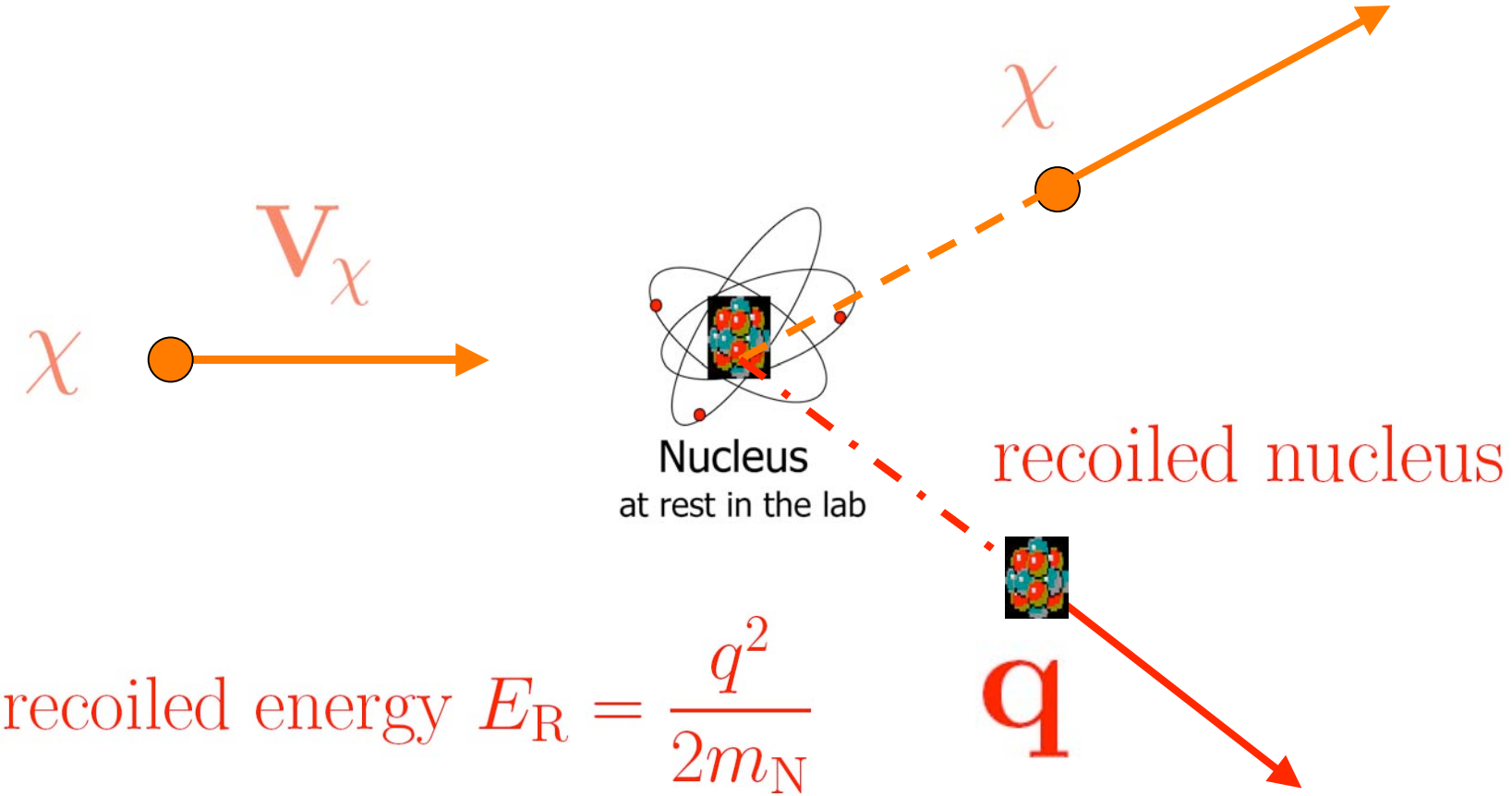

recoiled energy $E_{\mathrm{R}} = \dfrac{q^2}{2m_{\mathrm{N}}}$

This is the signal !

Center of Mass Frame

The CMF is defined by $(m_{\rm N} + m_\chi)\mathbf{V}_{\rm CMF} = m_\chi \mathbf{V}_\chi$

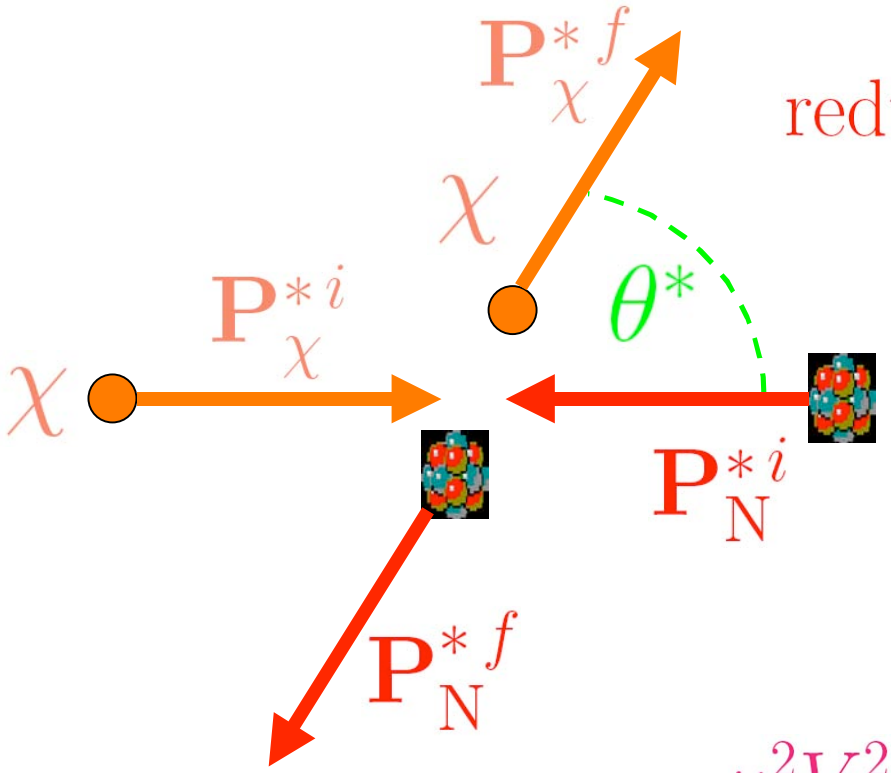

reduced mass $\mu = \dfrac{m_\chi m_{\rm N}}{m_\chi + m_{\rm N}}$

$P^* = \mu V_\chi$

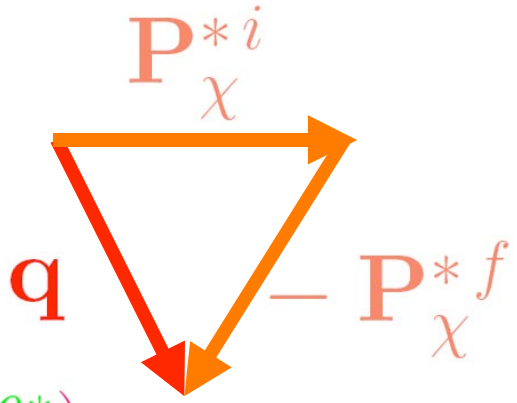

$$E_{\rm R} = \frac{\mu^2 V_\chi^2}{m_{\rm N}}(1 - \cos\theta^*)$$

$m_\chi = m_{\rm N} = 100$ GeV & $V_\chi = 220$ km s^{-1} yield $E_{\rm R}^{\rm max} \simeq 27$ keV

A (not too) naive toy model

$$\mathcal{L}_{\rm scalar} = A\, g_S\, \{\bar{\chi}\chi\}\cdot\{\bar{\Psi}_{\rm N}\Psi_{\rm N}\}$$

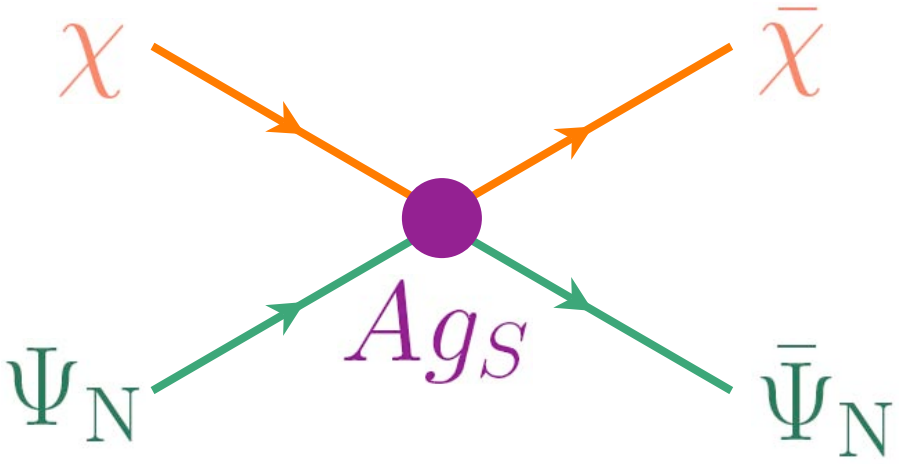

- Coherent interaction on the A nucleons of the nucleus N
- Effective scalar coupling $g_S \sim \dfrac{\alpha_{\rm em}}{M^2}$

$g_S \sim 7.3 \times 10^{-9}$ GeV^{-2} for a scale $M = 1$ TeV

Exercise – Level **[3]** *:* *The cross section for the scattering process*

$$\chi\,(P_1)\;+\;\text{nucleus}\,(k_1)\longrightarrow\chi\,(P_2)\;+\;\text{nucleus}\,(k_2)\quad,\tag{1}$$

is generically given by the well–known relation

$$d\sigma\cdot|\mathbf{V}_\chi-\mathbf{V}_{\rm N}|\;=\;\frac{1}{2\,P_1^0}\,\frac{1}{2\,k_1^0}\int d\tilde{P}_2\;d\tilde{k}_2\;(2\pi)^4\,\delta(P_1+k_1-P_2-k_2)\;\mathcal{A}\quad,\tag{2}$$

where $\mathcal{A}$ *denotes the average over the initial spin states and the sum over the final spin states of the square of the amplitude. Show that the later may be expressed as*

$$\mathcal{M}_{\,\rm scalar}\;=\;\sqrt{\kappa}\cdot A\,g_S\cdot\bar{u}(P_2)u(P_1)\cdot\bar{u}(k_2)u(k_1)\quad.\tag{3}$$

The κ *coefficient is equal to 1 for Dirac fermions and to 4 for Majorana species. In the NR limit where the velocities of the particles are negligible with respect to their energies, establish that* $\mathcal{A}$ *is given by*

$$\mathcal{A}\equiv\frac{1}{4}\sum_{\rm spins}|\mathcal{M}_{\,\rm scalar}|^2\;=\;16\,\kappa\,A^2\,g_S^2\,m_\chi^2\,m_{\rm N}^2\quad.\tag{4}$$

Compute the integral (2) in order to derive the differential cross section in the CMF

$$\frac{d\sigma}{d\Omega^*}\;=\;\frac{\kappa}{4\pi^2}\,A^2\,g_S^2\,\mu^2\quad.\tag{5}$$

A few consequences ensue

(i) Because the scattering is **isotropic** in the CMF, the differential cross section is **flat** as a function of the recoil energy $E_{\rm R}$

$$\sigma \;=\; \frac{\kappa}{\pi}\, A^2\, g_S^2\, \mu^2$$

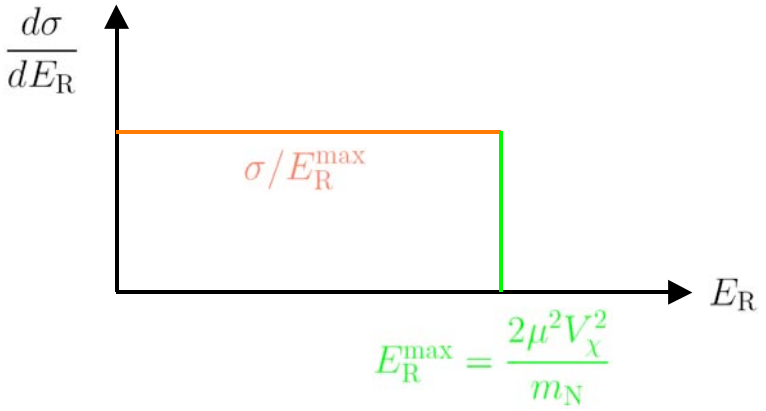

(ii) In order to compare among the various experiments, the **spin independent** cross section on a **single nucleon** is defined as

$$\sigma_{\rm p}^{\rm SI} = \lim_{m_\chi \to \infty} \sigma\left\{m_{\rm N} = m_{\rm p}, m_\chi\right\} = \frac{\kappa}{\pi}\, g_S^2\, m_{\rm p}^2$$

$$\sigma_{\rm p}^{\rm SI} \sim 23.3 \text{ zeptobarns}^* \text{ for a scale } M = 1 \text{ TeV}$$

(iii) The total scattering cross section varies with the atomic number A of the target nucleus as

$$\frac{\sigma}{\sigma_{\rm p}^{\rm SI}} \;=\; A^4 \left\{1 + \frac{m_{\rm N}}{m_\chi}\right\}^{-2} \longrightarrow A^4 \text{ when } m_\chi \gg m_{\rm N}$$

$*$ 1 zeptobarn (zp) $= 10^{-9}$ picobarn $= 10^{-45}$ cm^2

The model of the isothermal sphere

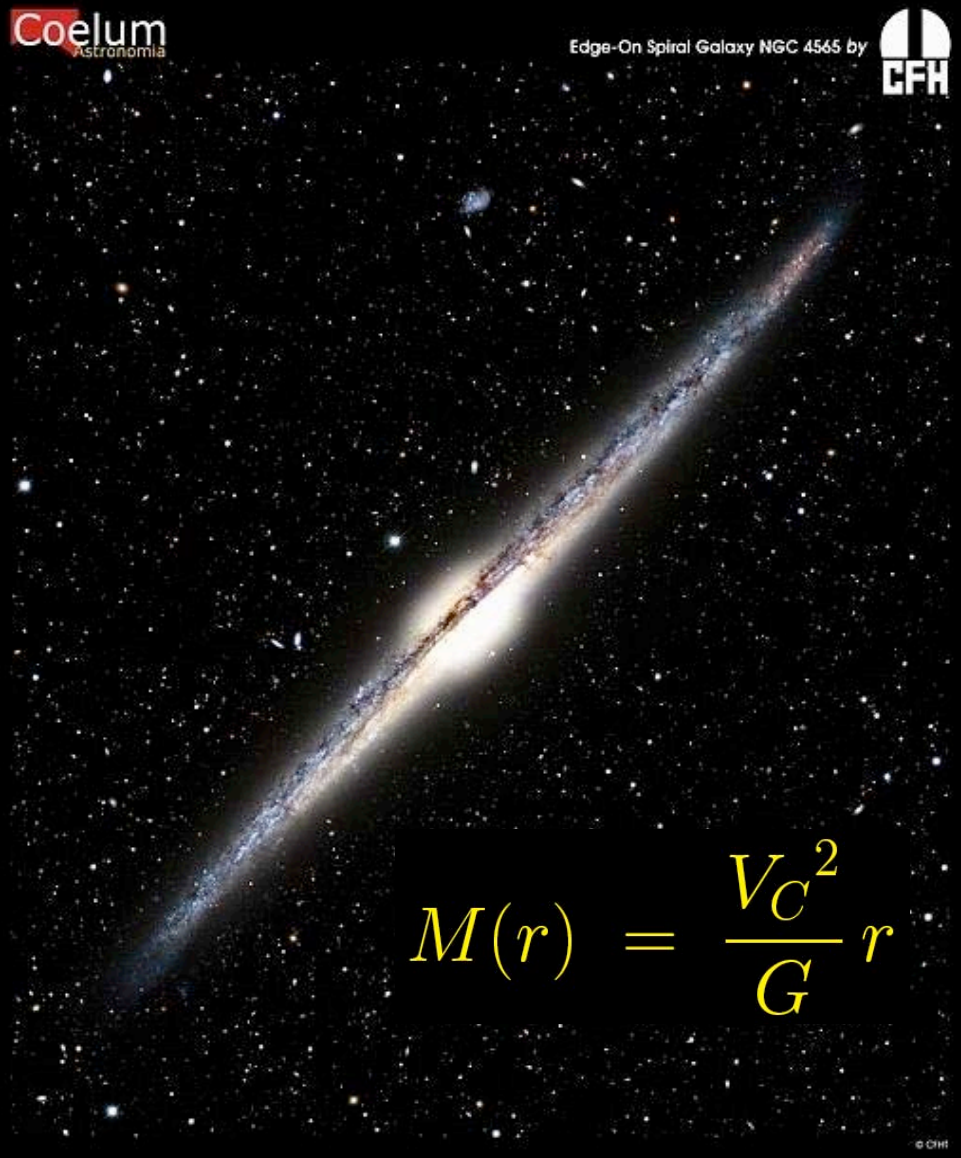

$$M(r) = \frac{{V_C}^2}{G} r$$

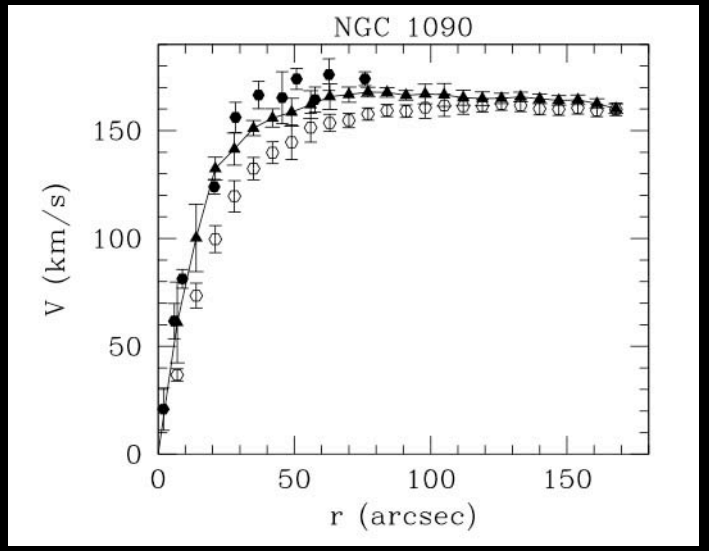

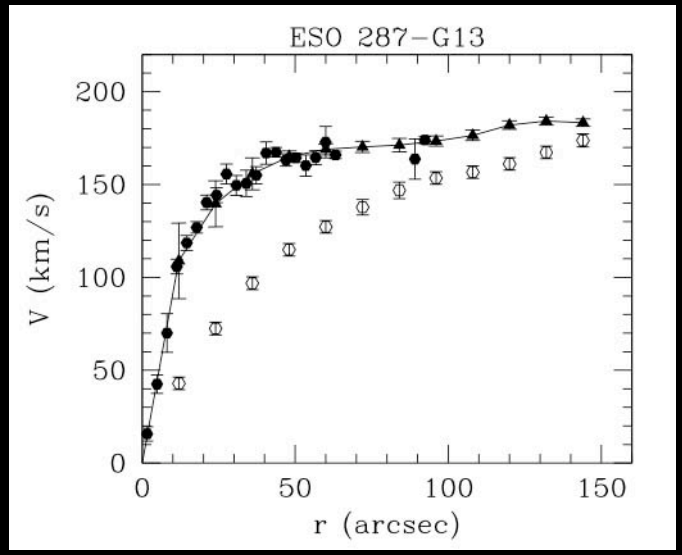

Exercise – Level **[2]** *:* *In the absence of collisions, point–like particles under the action of the gravitational potential* Φ *behave in phase–space like an incompressible fluid whose density* $\mathrm{f}(\mathbf{r}, \mathbf{v}, t)$ *follows the* **Vlasov** *equation*

$$\frac{\partial \mathrm{f}}{\partial t} + (\mathbf{v} \cdot \nabla)\,\mathrm{f} - (\nabla\Phi \cdot \nabla_v)\,\mathrm{f} = 0 \quad . \tag{1}$$

Show that any function f *of the mechanical energy per unit mass* $E = v^2/2 + \Phi(\mathbf{r})$ *is a stationary solution of (1). Let us choose the Maxwell–Boltzmann distribution* $f = C\,\exp(-E/\nu^2)$*, where* ν *denotes the typical velocity dispersion of the particles. By integrating out the velocities, establish that the mass density is given by*

$$\rho\,(\mathbf{r}) = \rho_c\,\exp\{-\,\Phi(\mathbf{r})/\nu^2\} \quad . \tag{2}$$

Assuming spherical symmetry, solve the Poisson equation

$$\Delta\Phi = \frac{1}{r^2}\,\frac{d}{dr}\left\{r^2\,\frac{d\Phi}{dr}\right\} = 4\,\pi\,G\,\rho(r) \quad . \tag{3}$$

for the scale invariant solution $\rho = A\,r^{\alpha}$*. Compute* A *and* α *in order to derive the specific form for the mass density of an isothermal sphere*

$$\rho(r) = \frac{\nu^2}{2\,\pi\,G}\,\frac{1}{r^2} \quad . \tag{4}$$

Show that if the dark matter inside a spiral galaxy follows that profile and if it dominates the dynamics of the system, the rotation curve is flat with velocity $V_C = \sqrt{2}\,\nu$*.*

The recoil spectrum

• The terrestrial detector is embedded inside a stream of neutralinos. Each nucleus may undergo a collision whose probability per unit time and unit of recoil energy is given by

$$\frac{\mathrm{d}\Gamma}{\mathrm{d}E_{\mathrm{R}}} = \frac{\rho_{\odot}}{m_{\chi}} \cdot \int_{v_{\mathrm{min}}(E_{\mathrm{R}})}^{v_{\mathrm{max}}} \mathrm{d}^3\mathbf{v}\ \mathrm{f}(\mathbf{v})\ v\ \frac{d\sigma}{dE_{\mathrm{R}}}$$

• In the limit where the recoil spectrum is flat, the rate of collision **per unit mass of the detector** may be expressed as the product

$$\frac{\mathrm{d}R}{\mathrm{d}E_{\mathrm{R}}} = \frac{\rho_{\odot}}{m_{\chi}} \cdot \frac{\sigma}{\sqrt{\pi}\mu^2 V_C} \cdot \mathcal{T}(E_R)$$

where the integral $\mathcal{T}(E_R)$ depends on the velocity distribution of the neutralinos

$$\mathcal{T}(E_R) = \frac{\sqrt{\pi}}{2} V_C \int_{v_{\mathrm{min}}(E_{\mathrm{R}})}^{v_{\mathrm{max}}} \frac{\mathrm{d}^3\mathbf{v}}{v}\ \mathrm{f}(\mathbf{v})$$

• DM particles need to have a large enough velocity in order to transfer the recoil energy E_R

$$E_{\rm R} = \frac{\mu^2 V_\chi^2}{m_{\rm N}}(1-\cos\theta^*)$$

$$\Downarrow$$

$$\frac{2\mu^2 v_{\rm min}^2}{m_{\rm N}} = E_R$$

• A **Maxwellian distribution** of velocity is assumed here for simplicity

$$\mathrm{f}(\mathbf{v}) = \left(\pi V_C^2\right)^{-3/2} \exp(-v^2/V_C^2)$$

$$\Downarrow$$

$$\mathcal{T}(E_R) = \exp(-v_{\rm min}^2/V_C^2)$$

$$\mathcal{T}(E_R) = \exp(-E_R/E_R^0) \text{ where } E_R^0 = 2\mu^2 V_C^2/m_{\rm N}$$

The recoil spectrum decreases exponentially with a variation scale set by E_R^0.
For ^{73}Ge and a 60 GeV neutralino, $E_R^0 = 16$ keV

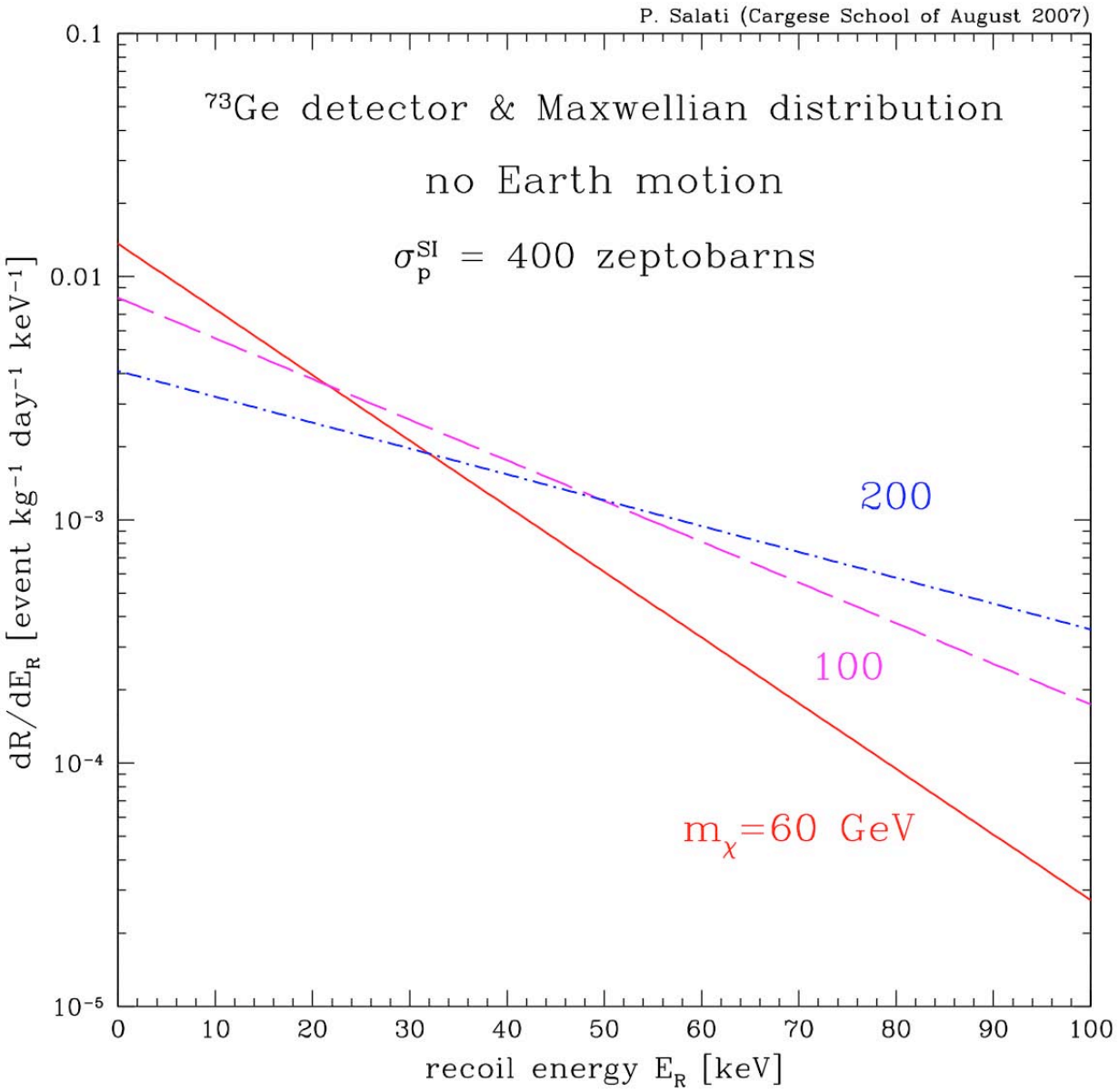
P. Salati (Cargese School of August 2007)
^{73}Ge detector & Maxwellian distribution
no Earth motion
σ_p^{SI} = 400 zeptobarns
200
100
m_χ=60 GeV
dR/dE$_R$ [event kg^{-1} day^{-1} keV^{-1}]
recoil energy E$_R$ [keV]
0.1
0.01
10^{-3}
10^{-4}
10^{-5}
0
10
20
30
40
50
60
70
80
90
100

Velocity distribution corrected for the Earth motion

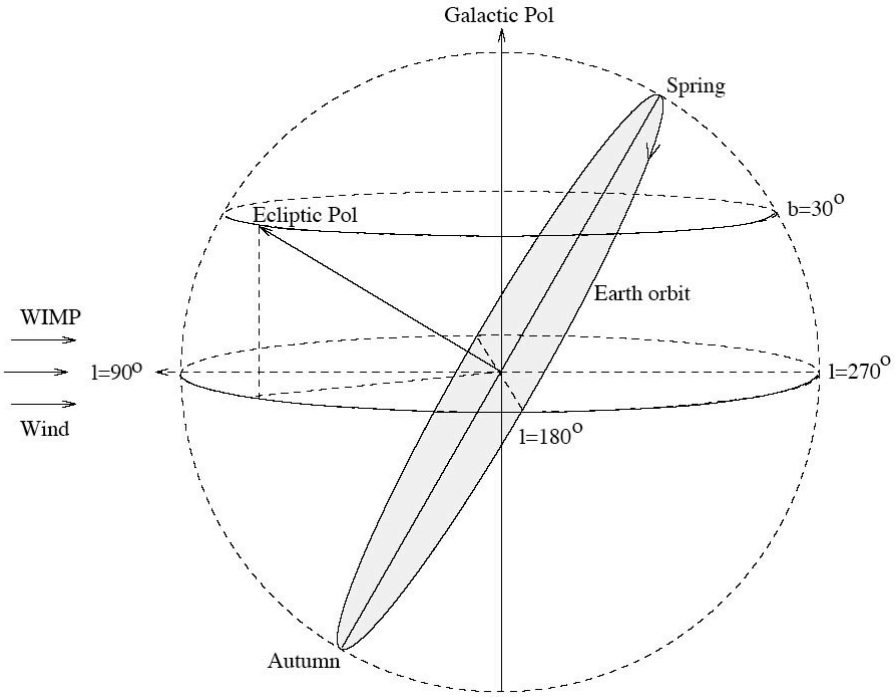

• The Earth moves actually in the Galactic frame and its velocity is of the same order of magnitude as V_C

$$v_e = V_C \cdot \left\{ 1.05 \; + \; 0.07 \cos \left\{ \frac{2\pi (t - t_P)}{1 \text{ yr}} \right\} \right\}$$

where t_P is June 2nd $\pm$ 1.3 days.

Velocity distribution corrected for the Earth motion

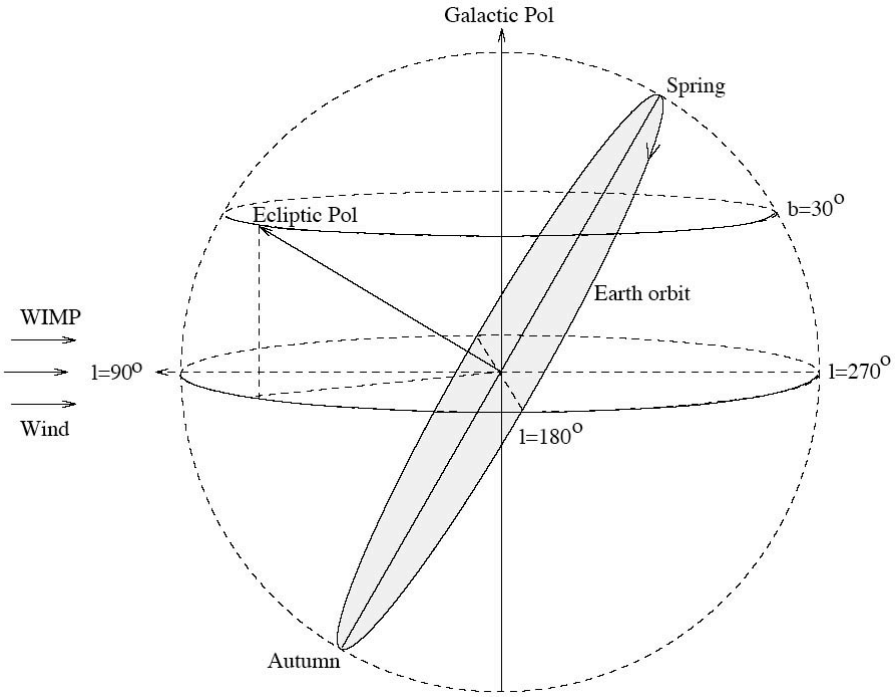

• As a consequence, if $\mathbf{v}$ denotes the neutralino velocity with respect to the Earth, the correct distribution is now given by the previous function f, where the argument $\mathbf{v}$ is replaced by the velocity $\mathbf{v}_{\rm G} = \mathbf{v} + \mathbf{v}_e$ as seen in the Galactic frame.

$$\mathcal{T}(E_R) = \frac{\sqrt{\pi}}{4} \cdot \frac{V_C}{v_e} \cdot \left\{ \mathrm{Erf}\left(\frac{v_{\rm min} + v_e}{V_C} \right) - \mathrm{Erf}\left(\frac{v_{\rm min} - v_e}{V_C} \right) \right\}$$

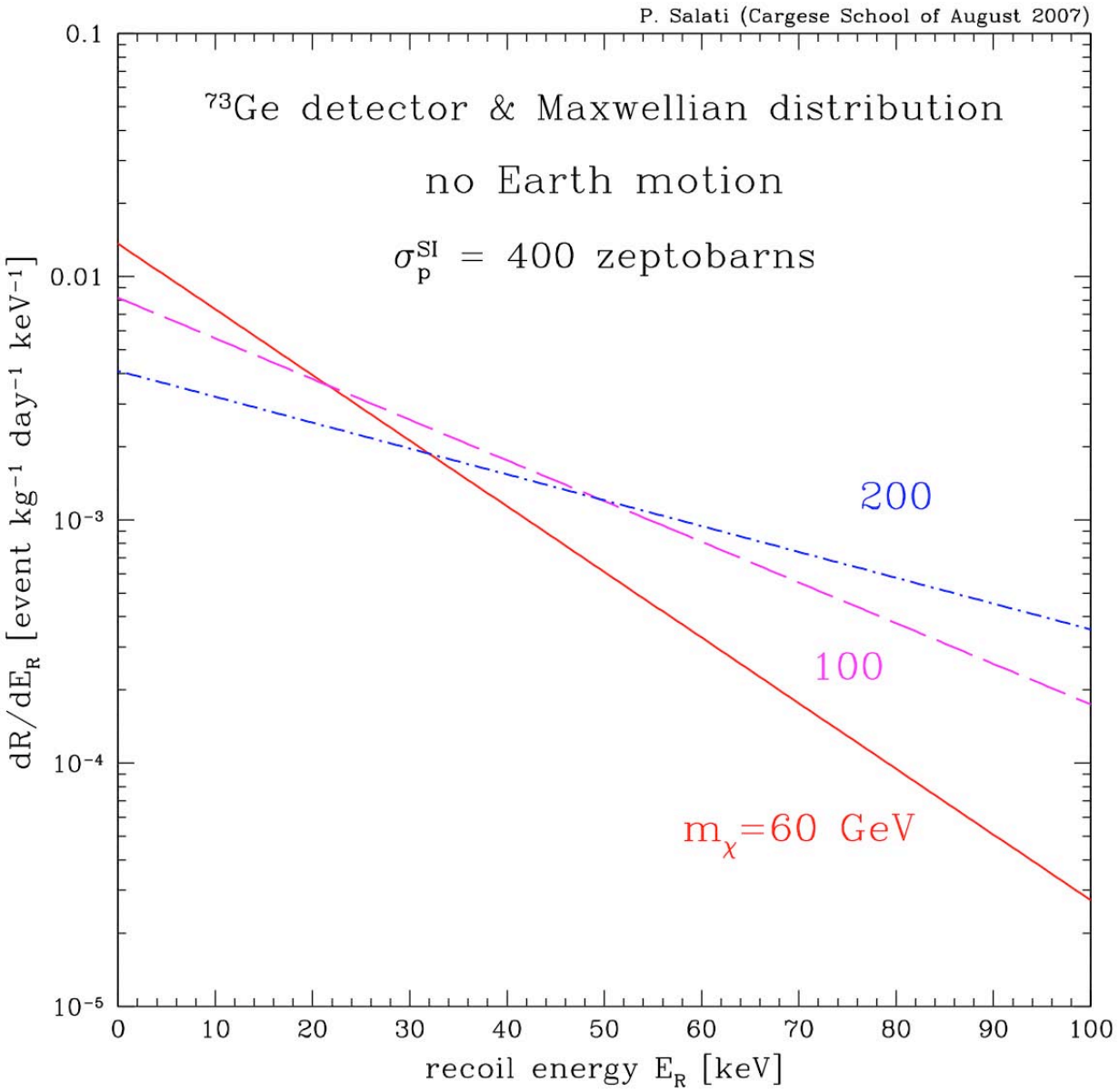
P. Salati (Cargese School of August 2007)
^{73}Ge detector & Maxwellian distribution
no Earth motion
σ_p^{SI} = 400 zeptobarns
200
100
m_χ=60 GeV
dR/dE$_R$ [event kg^{-1} day^{-1} keV^{-1}]
recoil energy E$_R$ [keV]
0.1
0.01
10^{-3}
10^{-4}
10^{-5}
0
10
20
30
40
50
60
70
80
90
100

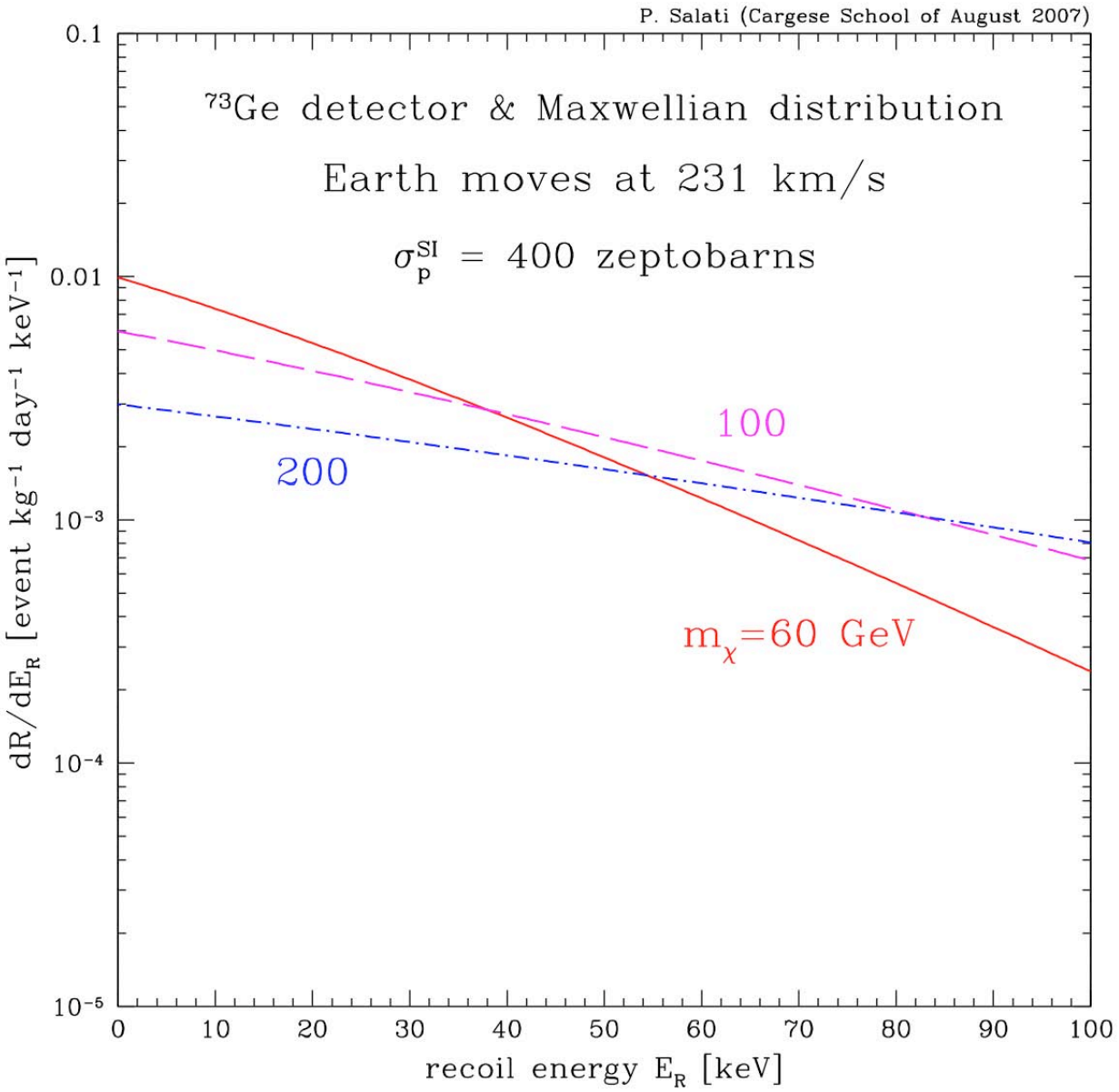
P. Salati (Cargese School of August 2007)
^{73}Ge detector & Maxwellian distribution
Earth moves at 231 km/s
σ_p^{SI} = 400 zeptobarns
100
200
m_χ=60 GeV
dR/dE$_R$ [event kg^{-1} day^{-1} keV^{-1}]
recoil energy E$_R$ [keV]
0.1
0.01
10^{-3}
10^{-4}
10^{-5}
0
10
20
30
40
50
60
70
80
90
100

Expected number of events $n_{\rm theo}$

- The exposure of the detector is defined as

$$\mathcal{E} = \text{Mass} \times \text{Duration}$$

and is expressed in units of kg $\times$ day.

- Events are detected above the threshold $E_{\rm th}$ up to an energy $E_{\rm max}$. During the period of observation – characterized by the exposure $\mathcal{E}$ – a number $n_{\rm theo}$ is expected

$$n_{\rm theo} = \mathcal{E} \times \int_{E_{\rm th}}^{E_{\rm max}} \frac{{\rm d}R}{{\rm d}E_{\rm R}} \, {\rm d}E_{\rm R}$$

- In the naive approach where the Earth motion is neglected and setting the upper bound $E_{\rm max}$ at infinity, the number of events simplifies into

$$n_{\rm theo} \simeq 4.14 \times 10^{-7} \text{ events kg}^{-1} \text{ day}^{-1} \times \left\{ \frac{\sigma_{\rm p}^{\rm SI}}{1\,\text{zb}} \right\} \times A^2 \times \left\{ \frac{\sqrt{x}-1}{x} \right\} \times e^{-\alpha x}$$

$$\text{where} \quad x = \left\{ 1 + \frac{m_{\rm N}}{m_\chi} \right\}^2 \quad \& \quad \alpha = \frac{E_{\rm th}}{2 m_{\rm N} V_C^2}$$

We require that $n_{\rm theo} \leq 2.3$ (90% CL for a null observation)

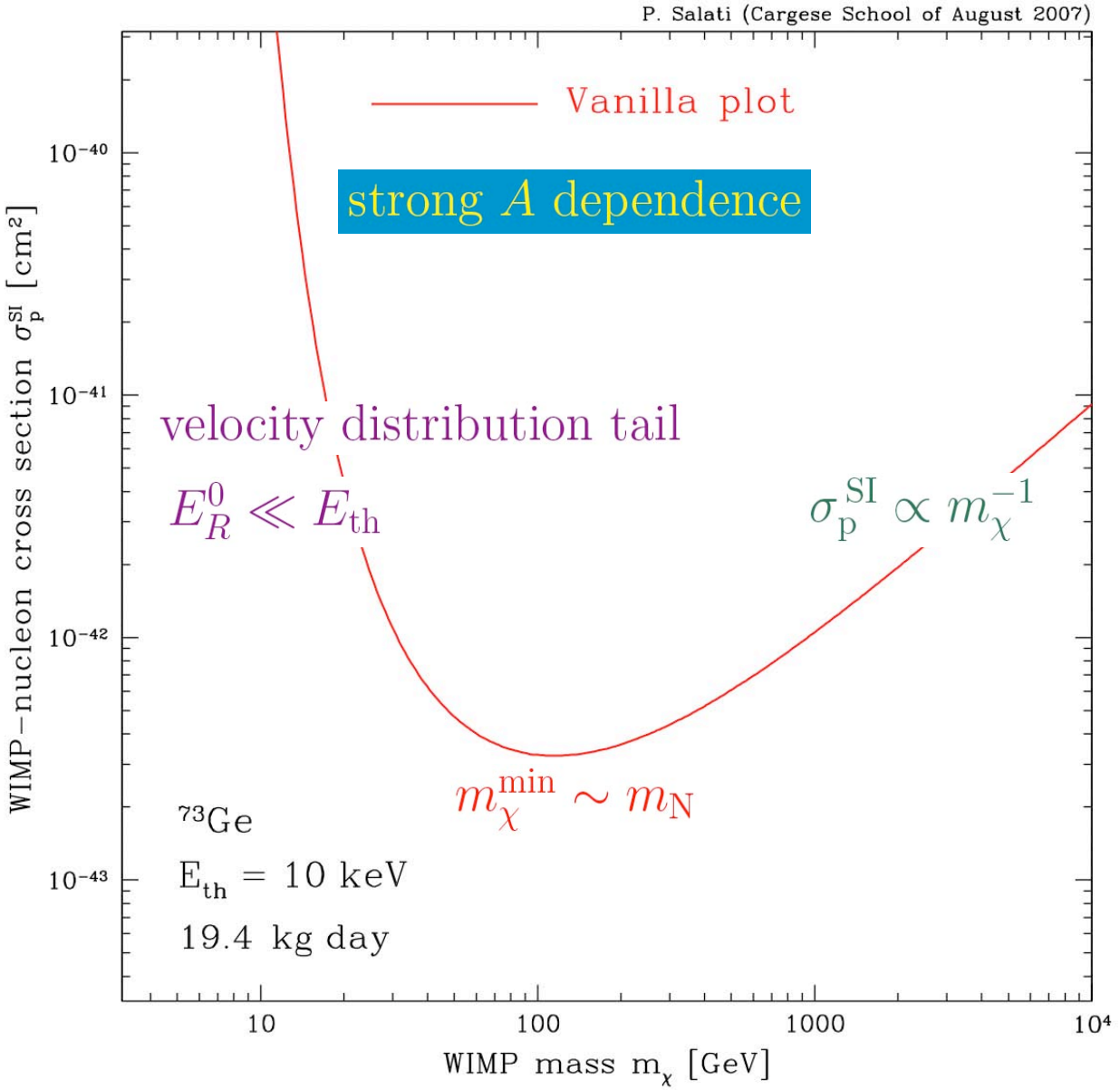

the heavier, the better !

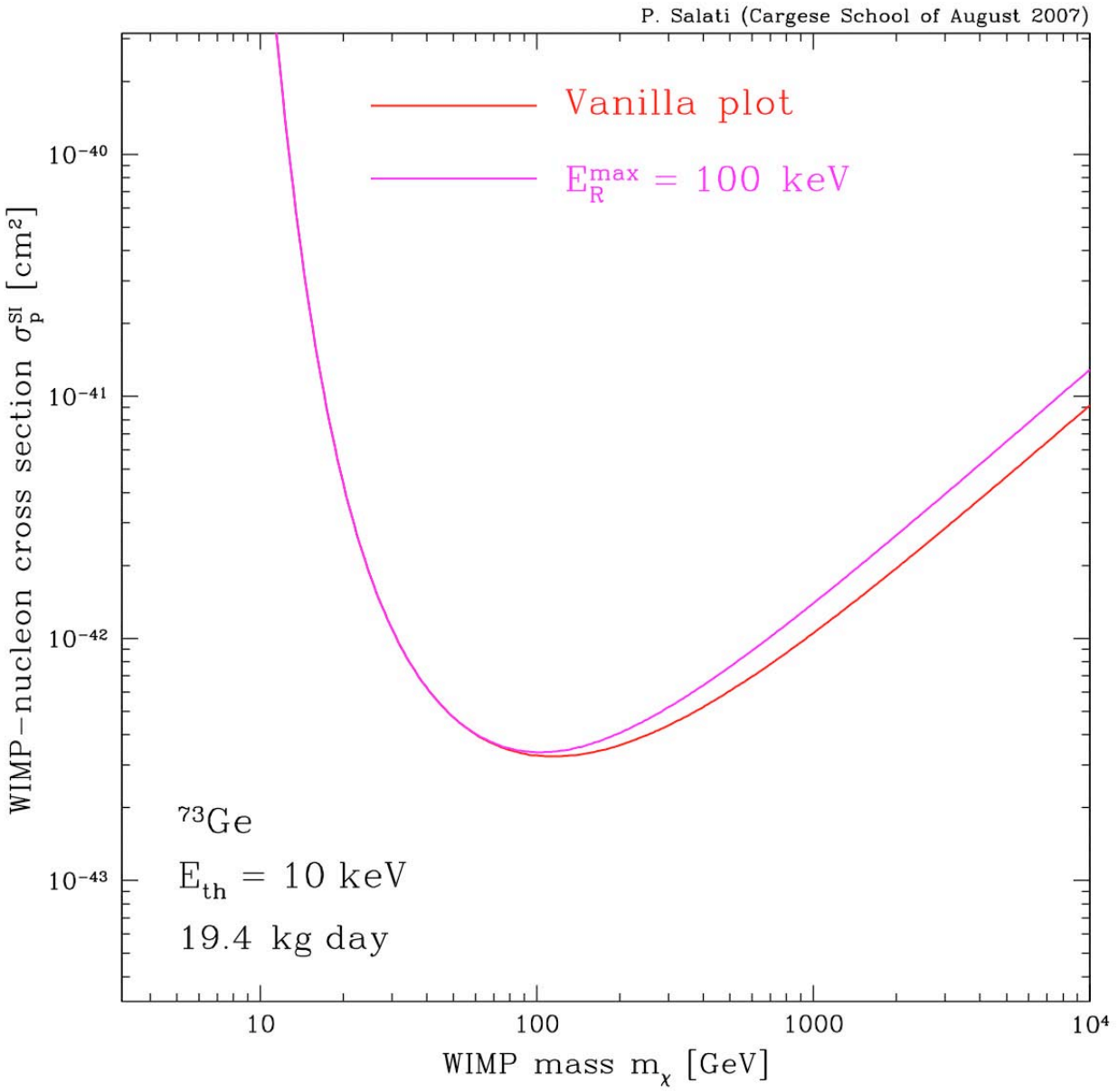
P. Salati (Cargese School of August 2007)
Vanilla plot
E_R^{max} = 100 keV
^{73}Ge
E_{th} = 10 keV
19.4 kg day
WIMP−nucleon cross section σ_p^{SI} [cm^2]
10^{-40}
10^{-41}
10^{-42}
10^{-43}
10
100
1000
10^4
WIMP mass m_χ [GeV]

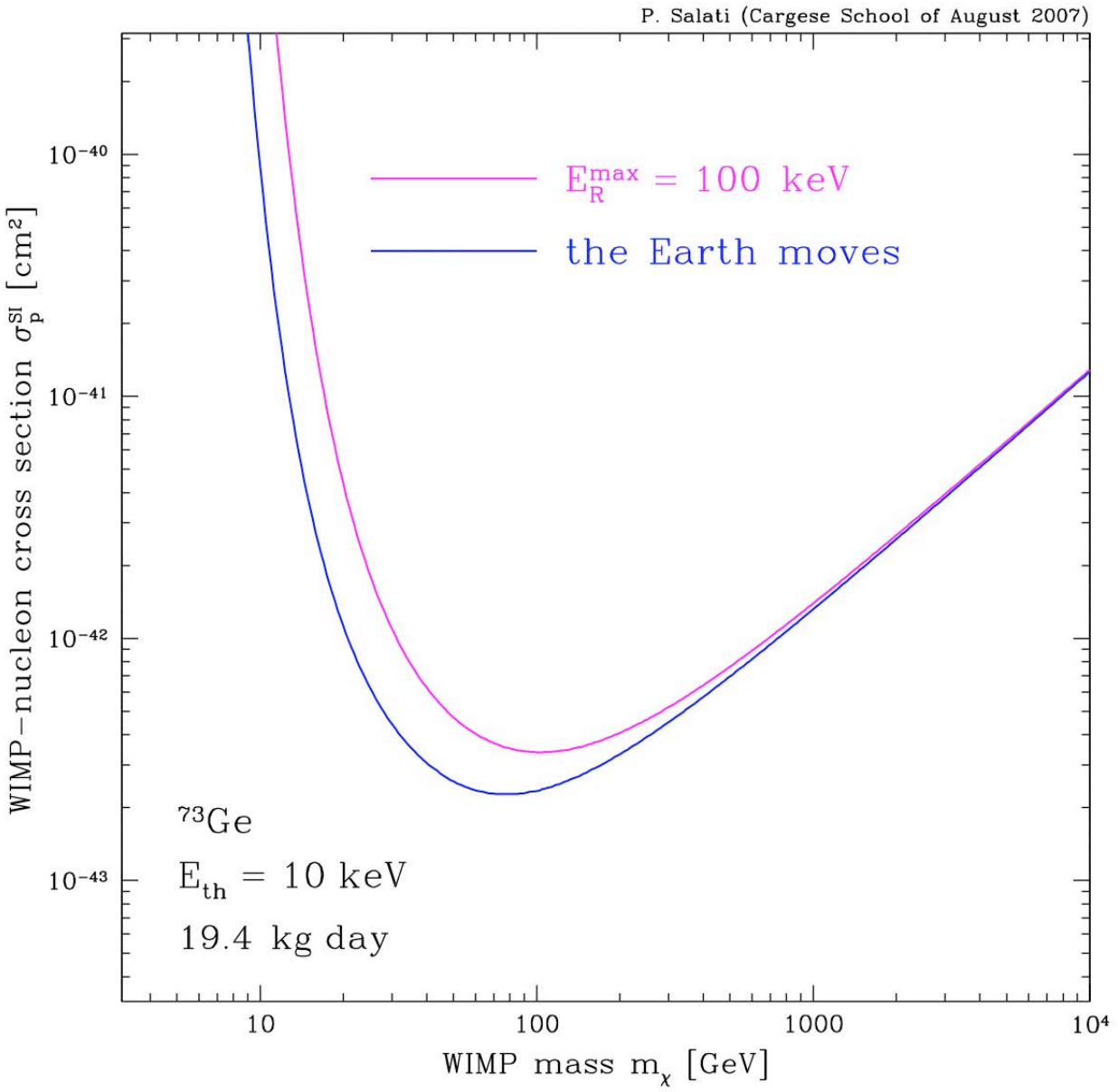
P. Salati (Cargese School of August 2007)
WIMP−nucleon cross section σ_p^{SI} [cm²]
10^{-40}
10^{-41}
10^{-42}
10^{-43}
E_R^{max} = 100 keV
the Earth moves
^{73}Ge
E_{th} = 10 keV
19.4 kg day
10
100
1000
10^4
WIMP mass m_χ [GeV]

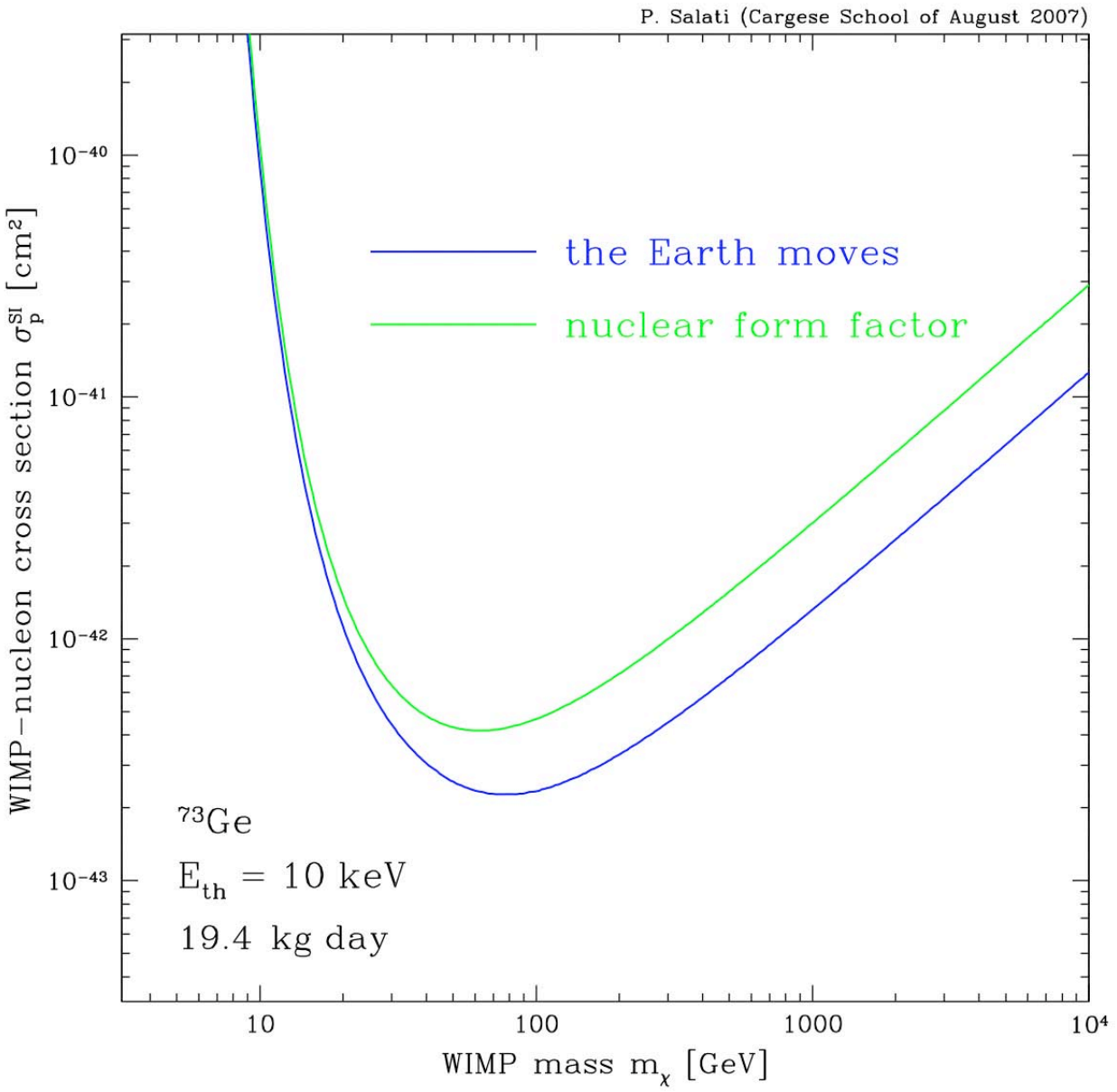
P. Salati (Cargese School of August 2007)
WIMP−nucleon cross section σ_p^{SI} [cm²]
10^{-40}
10^{-41}
10^{-42}
10^{-43}
the Earth moves
nuclear form factor
^{73}Ge
E_{th} = 10 keV
19.4 kg day
10
100
1000
10^4
WIMP mass m_χ [GeV]

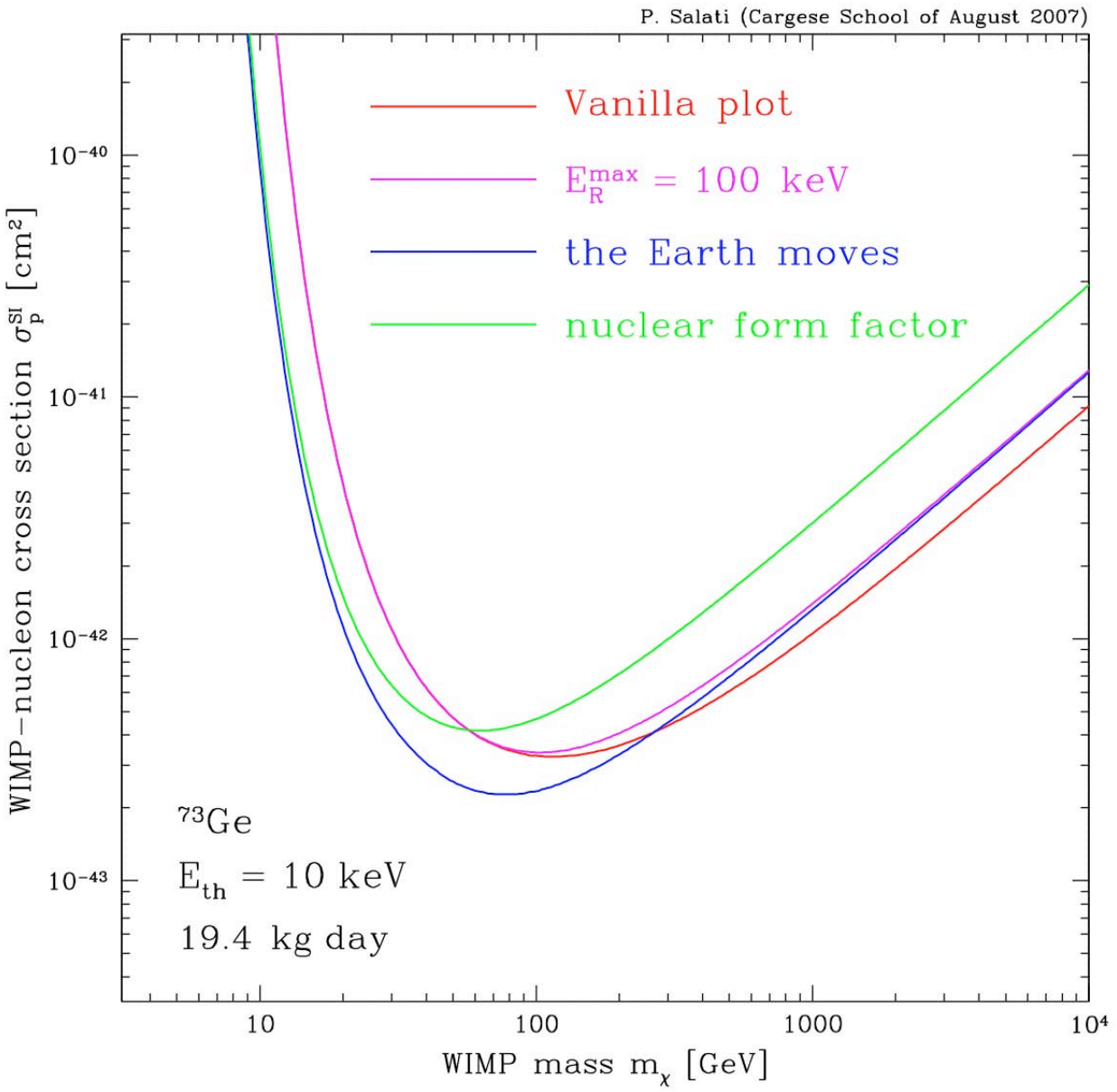
P. Salati (Cargese School of August 2007)
Vanilla plot
E_R^{max} = 100 keV
the Earth moves
nuclear form factor
^{73}Ge
E_{th} = 10 keV
19.4 kg day
WIMP−nucleon cross section σ_p^{SI} [cm^2]
10^{-40}
10^{-41}
10^{-42}
10^{-43}
10
100
1000
10^4
WIMP mass m_χ [GeV]

Effect of the atomic number A

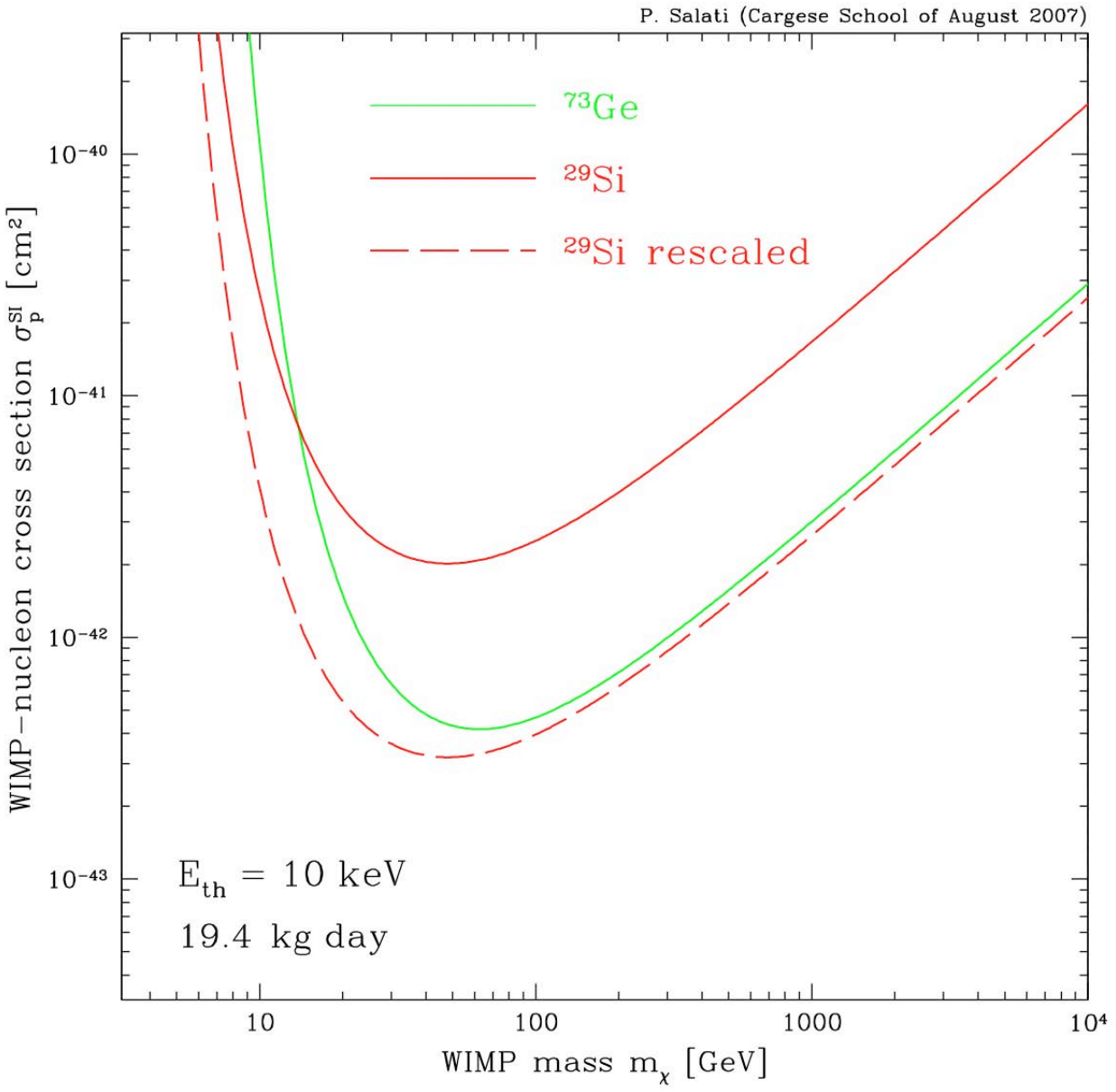

Effect of the atomic number A

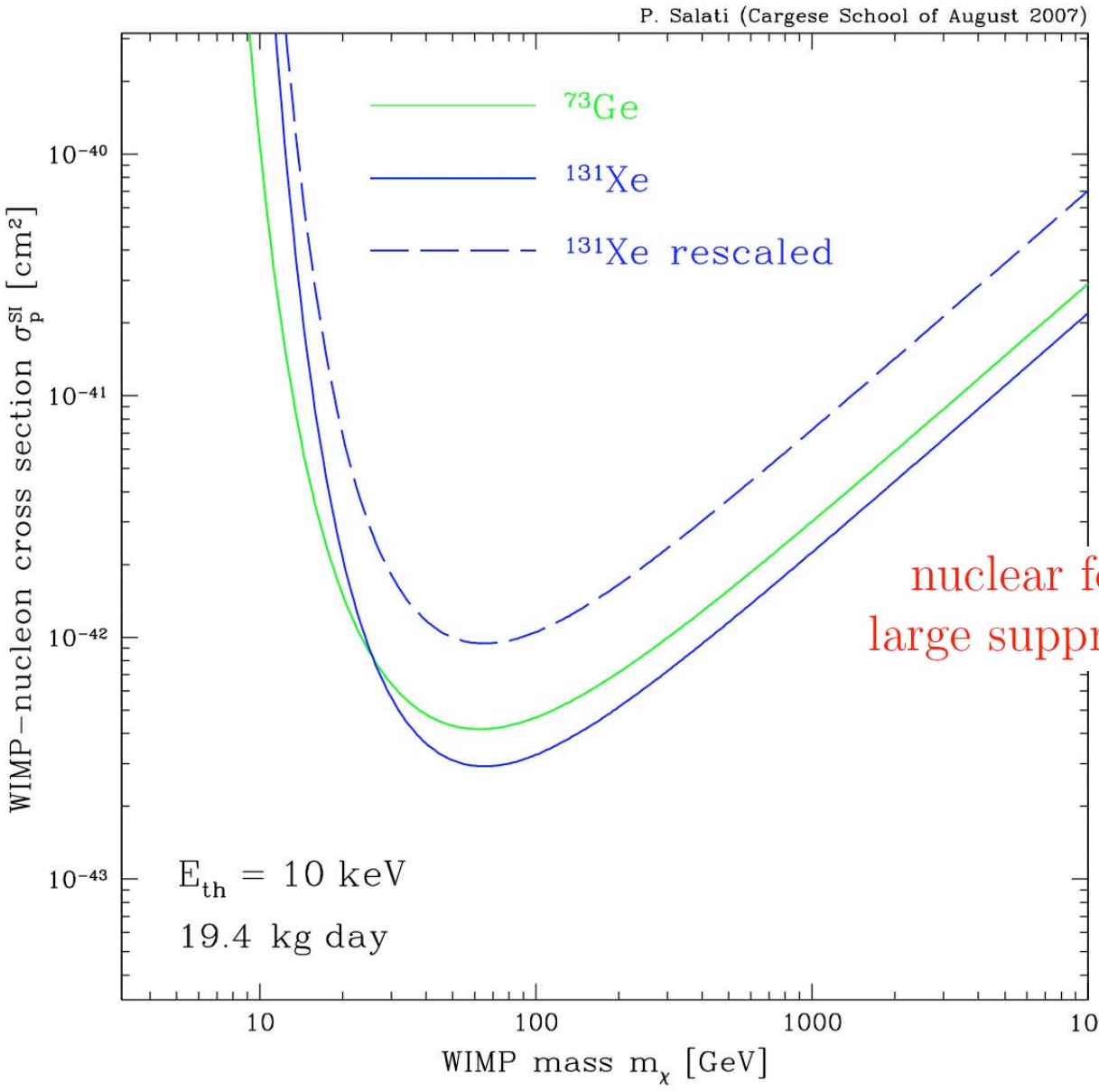

nuclear form factor
large suppression effect

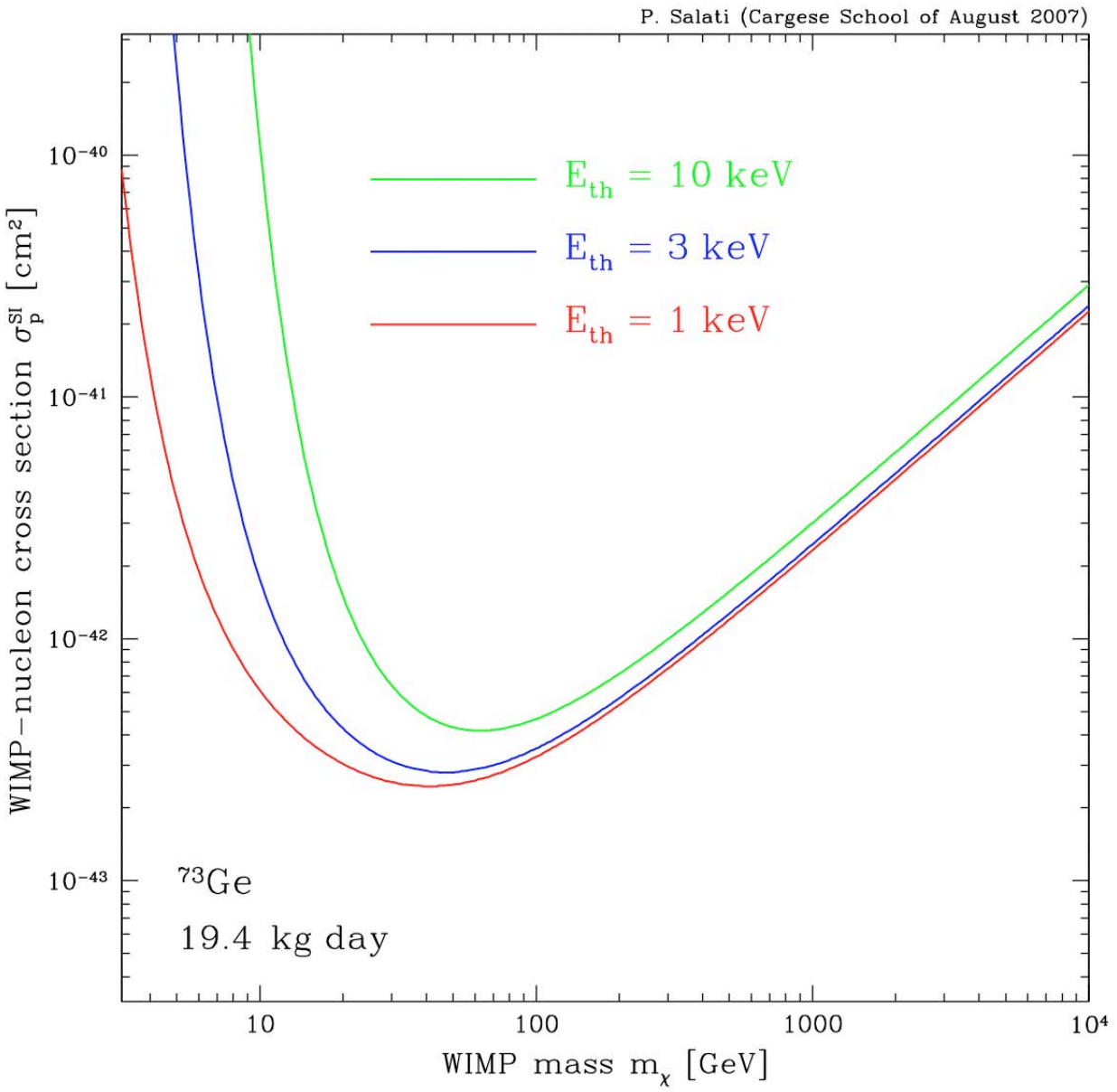
P. Salati (Cargese School of August 2007)
E_{th} = 10 keV
E_{th} = 3 keV
E_{th} = 1 keV
^{73}Ge
19.4 kg day
WIMP−nucleon cross section σ_p^{SI} [cm^2]
WIMP mass m_χ [GeV]
10^{-40}
10^{-41}
10^{-42}
10^{-43}
10
100
1000
10^4

1 ton × 10 days to reach the ZB level

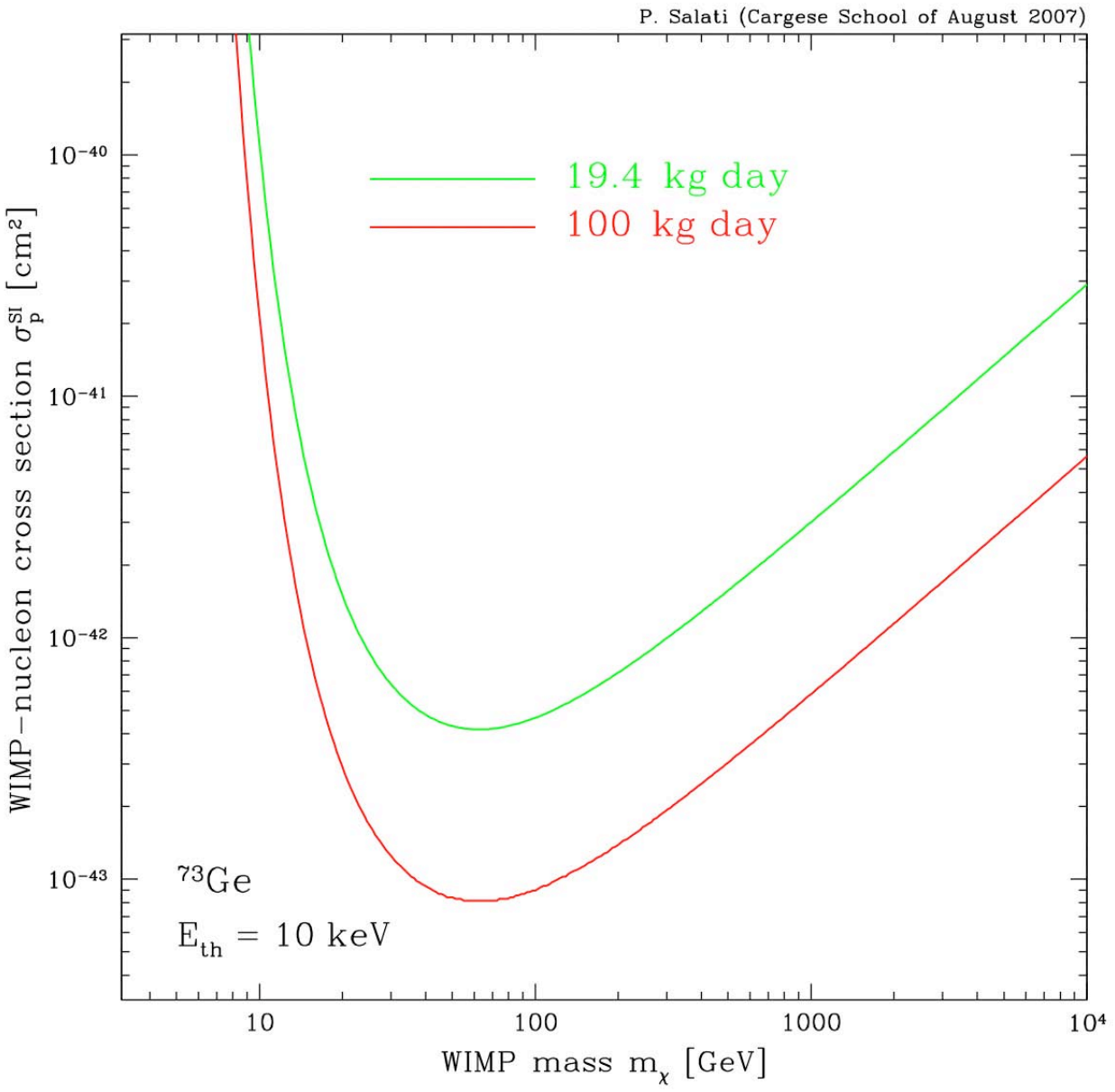

Direct Dark Matter Detection

Pierre Salati – Université de Savoie & **LAPTH**

1) Collision kinematics and the nucleus recoil

2) Scattering cross section and nucleon content

3) The experimental measurements and astrophysics

4) Future prospects

Cosmology and Particle Physics Beyond the Standard Models – Cargese – August 7, 2007

Exercise – Level **[3]** *: Let us consider the effective neutralino–neutralino vertex*

$$\mathcal{L}_{\rm eff} = \bar{\chi}\,\Gamma\,\chi \ , \tag{1}$$

where Γ stands for some combination of Dirac matrices. In direct detection, the amplitude of the diffusion implies the matrix element $\langle\, 2\,|\,\bar{\chi}\,\Gamma\,\chi\,|\,1\,\rangle$. A neutralino with initial momentum P_1 scatters on a nucleus and gets the momentum P_2. In supersymmetry, the neutralino is a **Majorana** *fermion. Both particle and antiparticle are one and the same species so that the corresponding field may be Fourier expanded as*

$$\chi(x) \ = \ \int \tilde{dk} \sum_{\alpha=1,2} \Big\{ a(\vec{k},\alpha)\, u(\vec{k},\alpha)\, e^{-\,ikx} \ + \ a^\dagger(\vec{k},\alpha)\, v(\vec{k},\alpha)\, e^{ikx} \Big\} \ . \tag{2}$$

Notice that both the creation a and annihilation $a^\dagger$ operators are present in χ and $\bar{\chi}$. Show that

$$\langle\, 2\,|\,\bar{\chi}\,\Gamma\,\chi\,|\,1\,\rangle = \bar{u}(2)\Gamma u(1) \ - \ \bar{v}(1)\Gamma v(2) \ . \tag{3}$$

The 4–spinors u and v are related though charge conjugation by $u = v^{\rm c} \equiv C\,\bar{v}^{\rm T}$ and C is equal to $i\gamma^2\gamma^0$ up to a phase in the 4–spinor Dirac representation. Infer from above that

$$\langle\, 2\,|\,\bar{\chi}\,\Gamma\,\chi\,|\,1\,\rangle = \bar{u}(2)\,\big\{\Gamma \ - \ C\,\Gamma^{\rm T} C\big\}\,u(1) \ . \tag{4}$$

Compute the previous expression for $\Gamma = 1$ (scalar), γ^μ (vector), $\sigma^{\mu\nu} = (i/2)[\gamma^\mu,\gamma^\nu]$ (tensor), $\gamma^5\gamma^\mu$ (axial) and γ^5 (pseudo–scalar). Show that the vector and tensor contributions vanish exactly. How does the pseudo–scalar contribution behave in the non–relativistic limit ?

The axial coupling $\mathcal{L}_{\rm A} = {\rm d}_q \cdot \bar{\chi}\gamma^\mu\gamma_5\chi \cdot \bar{q}\gamma_\mu\gamma_5 q$

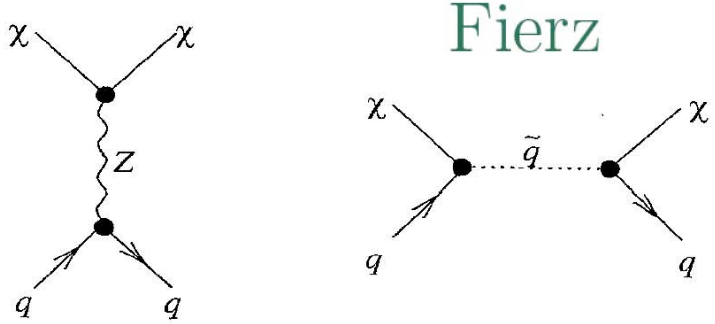

Fig. 19. Feynman diagrams contributing to the spin-dependent elastic scattering of neutralinos from quarks.

A.1) Once a particular SUSY model has been selected, the microscopic couplings ${\rm d}_q$ are fixed. The matrix element of the above quark axial–vector current in a nucleon – neutron or proton – may be extracted from data on polarized deep–inelastic scattering

$$\langle\, n \,|\, \bar{q}\,\gamma_\mu\gamma_5\, q \,|\, n \,\rangle \;=\; 2\; s_\mu^{(n)}\; \Delta q^{(n)}$$

$$\Downarrow$$

$$\mathcal{L}_{\rm A} = \bar{\chi}\gamma^\mu\gamma_5\chi \cdot \bar{n}\, s_\mu n \cdot \left\{ \sum_{\rm u,d,s} 2\; {\rm d}_q\, \Delta q^{(n)} \equiv 2\sqrt{2}\, G_F^2\, a_{(n)} \right\}$$

Current picture of the proton

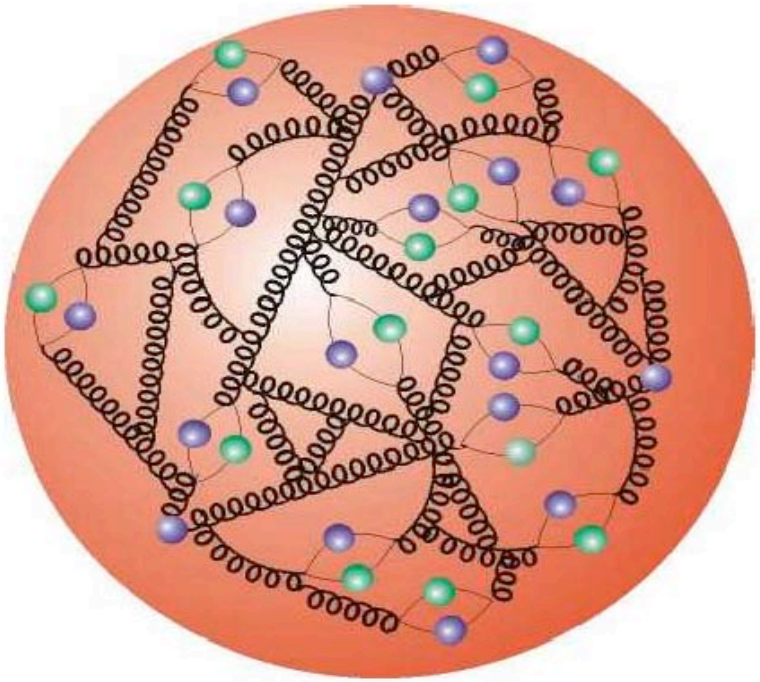

Table 3
Quark spin content of the proton determined from the SU(3) naive quark model (NQM) [9, 271, 272] and for measured spin-dependent structure functions from EMC [270, 273], SMC [274], and a compilation (All) [274]. Also listed are values using the 1σ error on $\Delta\Sigma$ from the compilation [296]

	NQM	EMC	SMC	All	$\text{All}_{\Delta\Sigma+1\sigma}$
Γ	0.188	0.137	0.136	0.145	0.145
$\Delta\Sigma$	0.60	0.12	0.22	0.30	0.42
$\Delta s^{(p)}$	0	− 0.16	− 0.12	− 0.09	− 0.09
$\Delta u^{(p)}$	0.93	0.78	0.74	0.77	0.73
$\Delta d^{(p)}$	− 0.33	− 0.50	− 0.40	− 0.38	− 0.22

G. Jungman, M. Kamionkowski & K. Griest, Physics Reports **267** (1996) 195–373

A.2) The next step is the calculation of the matrix elements of the nucleon spin operators $(\bar{n}\, s_\mu n)$ in the **nuclear** state $|\,\mathrm{N}\,\rangle$. At zero momentum transfer $\mathbf{q}$, this translates into the evaluation of the average proton spin $\langle S_\mathrm{p}\rangle$ and neutron spin $\langle S_\mathrm{n}\rangle$ inside the target nucleus

$$\mathcal{L}_\mathrm{A} \propto \{a_\mathrm{p}\,\langle S_\mathrm{p}\rangle + a_\mathrm{n}\,\langle S_\mathrm{n}\rangle \equiv \Lambda\, J\}$$

$$\Downarrow$$

$$\frac{d\sigma}{d|\mathbf{q}|^2} = \frac{8}{\pi}\,\frac{G_F^2}{v^2}\,\Lambda^2\, J(J+1)$$

Table 4
Comparison of odd-group model results with best estimates from more detailed calculations. EOGM is the extended odd-group model, and IBFM is the interacting–boson–fermion model

Nucleus	$\langle S_p\rangle_{OGM}$	$\langle S_n\rangle_{OGM}$	$\langle S_p\rangle$	$\langle S_n\rangle$	Model [Ref.]
^{19}F	0.46	0.0	0.415	− 0.047	EOGM1 [23]
			0.368	− 0.001	EOGM2 [23]
^{27}Al	0.25	0.0	− 0.343	0.030	Shell model [321]
^{29}Si	0.0	0.15	− 0.002	0.13	Shell model [269]
^{35}Cl	− 0.15	0.0	− 0.094	0.014	EOGM1 [23]
			− 0.083	0.004	EOGM2 [23]
^{39}K	− 0.24	0.0	− 0.18	0.05	Perturbation theory [321]
^{73}Ge	0.0	0.23	0.011	0.491	Shell model [269]
			0.030	0.378	Hybrid [276]
^{93}Nb	0.36	0.0	0.46	0.08	Shell model [275]
^{131}Xe	− 0.041	− 0.236	0.0	− 0.166	IBFM [419, 296]

A.3) The impinging WIMP probes the nuclear structure on a distance

$$\lambda \sim q^{-1} \sim 1/\sqrt{2 m_{\rm N} E_R}$$

that may be smaller than the nucleus size. For ^{131}Xe and a recoil energy of 100 keV, the diffraction scale is $\sim$ 1 fermi. A form factor should be introduced in the cross section

$$\frac{d\sigma}{d|\mathbf{q}|^2} = \frac{8}{\pi} \frac{G_F^2}{v^2} \Lambda^2 \, J(J+1) \left\{ \frac{S(q)}{S(0)} \right\}$$

The neutralino–proton and neutralino–neutron couplings can be rearranged into an isoscalar ($a_0 = a_{\rm p} + a_{\rm n}$) and an isovector ($a_1 = a_{\rm p} - a_{\rm n}$) part to yield

$$S(q) = a_0^2 \, S_{00}(q) \; + \; a_0 \, a_1 \, S_{01}(q) \; + \; a_1^2 \, S_{11}(q)$$

Large uncertainties !

The scalar coupling $\mathcal{L}_S \supset \lambda_q \cdot \bar{\chi}\chi \cdot \bar{q}q$

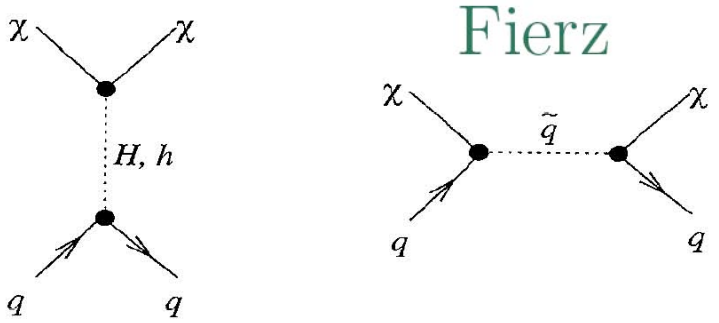

Fig. 20. Feynman diagrams contributing to the scalar elastic-scattering amplitude of a neutralino from quarks.

S.1) The microscopic scalar coupling of neutralinos to quarks is given at tree level by a Higgs and a squark exchange. Neutralinos couple also to gluons through a quark/squark loop. The tensor couplings $\bar{\chi}(i\partial_\mu\gamma_\nu + i\partial_\nu\gamma_\mu)\chi$ and $\bar{\chi}\partial_\mu\partial_\nu\chi$ arise finally from twist–two operators. **In order to simplify the discussion, we will concentrate only on the tree level diagrams with couplings $\lambda_q \propto m_q$.** The first step is to evaluate the neutralino–nucleon effective coupling

$$\mathcal{L}_S^{\text{eff}} = \sum_{\text{quarks}} \frac{\lambda_q}{m_q} \cdot \langle\, n \,|\, m_q\, \bar{q}q \,|\, n \,\rangle \cdot \bar{\chi}\chi$$

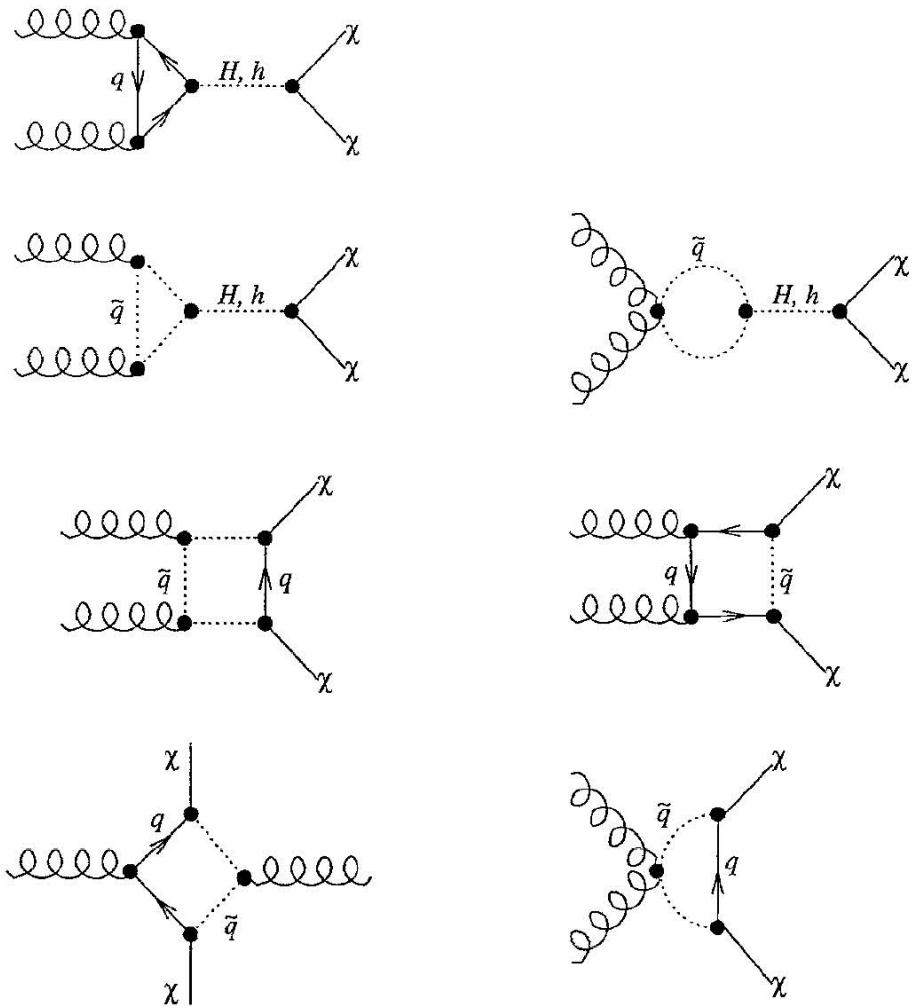

Fig. 21. Feynman diagrams contributing to the gluonic interaction with neutralinos, which contributes to the scalar elastic-scattering amplitude for neutralinos from nuclei.

S.2) The matrix elements of the light quarks can be derived in chiral perturbation theory from the determination of the pion–nucleon sigma term $\sigma_{\pi N}$ whose value is not known precisely (between 45 to 60 MeV). **This will come out to be the main source of uncertainty in the calculation of the effective neutralino–nucleon coupling.**

$$\langle n \,|\, m_q \bar{q} q \,|\, n \rangle = m_n \, f_{Tq}^{(n)}$$

Estimates for the nucleon parameters f_{Tq}. The u- and d-quark values are obtained from Ref. [284], and we list values reported for f_{Ts} by several authors

Nucleon	f_{Tu}	f_{Td}	f_{Ts} [285]	F_{Ts} [283, 284]	F_{Ts} [288]
n	0.023	0.034	0.14	0.46	0.08
p	0.019	0.041	0.14	0.46	0.08

S.3) In order to complete the calculation, two key ingredients are necessary.

- The nucleon mass is given by the trace of the QCD energy–momentum tensor

$$m_n = \langle n \,|\, \left\{ \Theta^{\mu}_{\mu} \equiv \sum_{\mathrm{u,d,s}} m_q \bar{q} q \; + \; \sum_{\mathrm{c,b,t}} m_Q \bar{Q} Q \; - \; \frac{7\alpha_S}{8\pi} GG \right\} \,|\, n \rangle$$

• In the limit where the quarks Q are heavy, their contributions to the nucleon mass, which occur through a loop diagram, may be expressed in terms of the gluonic content

$$\langle\, n \,|\, m_Q\, \bar{Q}Q \,|\, n \,\rangle \equiv -\,\frac{2\alpha_S}{24\pi}\, \langle\, n \,|\, GG \,|\, n \,\rangle$$

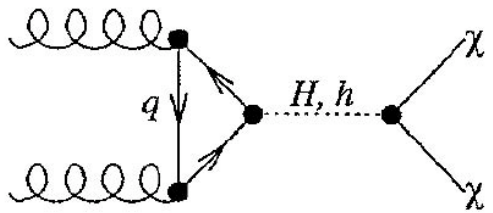

$\mathcal{L}_S^{\rm eff} = f_{(n)} \cdot (\bar{n}\, n) \cdot (\bar{\chi}\chi)$ where

$$f_{(n)} = m_n \left\{ \sum_{\rm u,d,s} \frac{\lambda_q}{m_q}\, f_{Tq}^{(n)} \;+\; \frac{2}{27} (1 - \sum_{\rm u,d,s} f_{Tq}^{(n)}) \sum_{\rm c,b,t} \frac{\lambda_Q}{m_Q} \right\}$$

The strange quark dominates

Large uncertainties !

S.4) For large enough transfer momenta q, the neutralino undergoes a diffraction on the nucleus and the scattering amplitude is modulated by the form factor

$$F(q) \equiv F(E_R) = \exp\left(-E_R/2Q_0\right)$$

The nuclear coherence energy $Q_0 = 1.5/(m_N R_0^2)$ depends on the radius R_0 of the nucleus

$$R_0 = 1 \text{ fermi} \times \left(0.3 + 0.9A^{1/3}\right)$$

The rate of detection is therefore reduced at large recoil energies and our (not so) naive estimate becomes

$$\frac{\mathrm{d}R}{\mathrm{d}E_\mathrm{R}} = \frac{\rho_\odot}{m_\chi} \cdot \frac{\sigma}{\sqrt{\pi}\mu^2 V_C} \cdot F^2(E_R) \cdot \mathcal{T}(E_R)$$

where the scalar cross section σ depends on the neutralino–proton f_p and neutralino–neutron f_n couplings

$$\sigma = \frac{4}{\pi}\mu^2 \left\{Z f_\mathrm{p} + (A-Z) f_\mathrm{n}\right\}^2$$

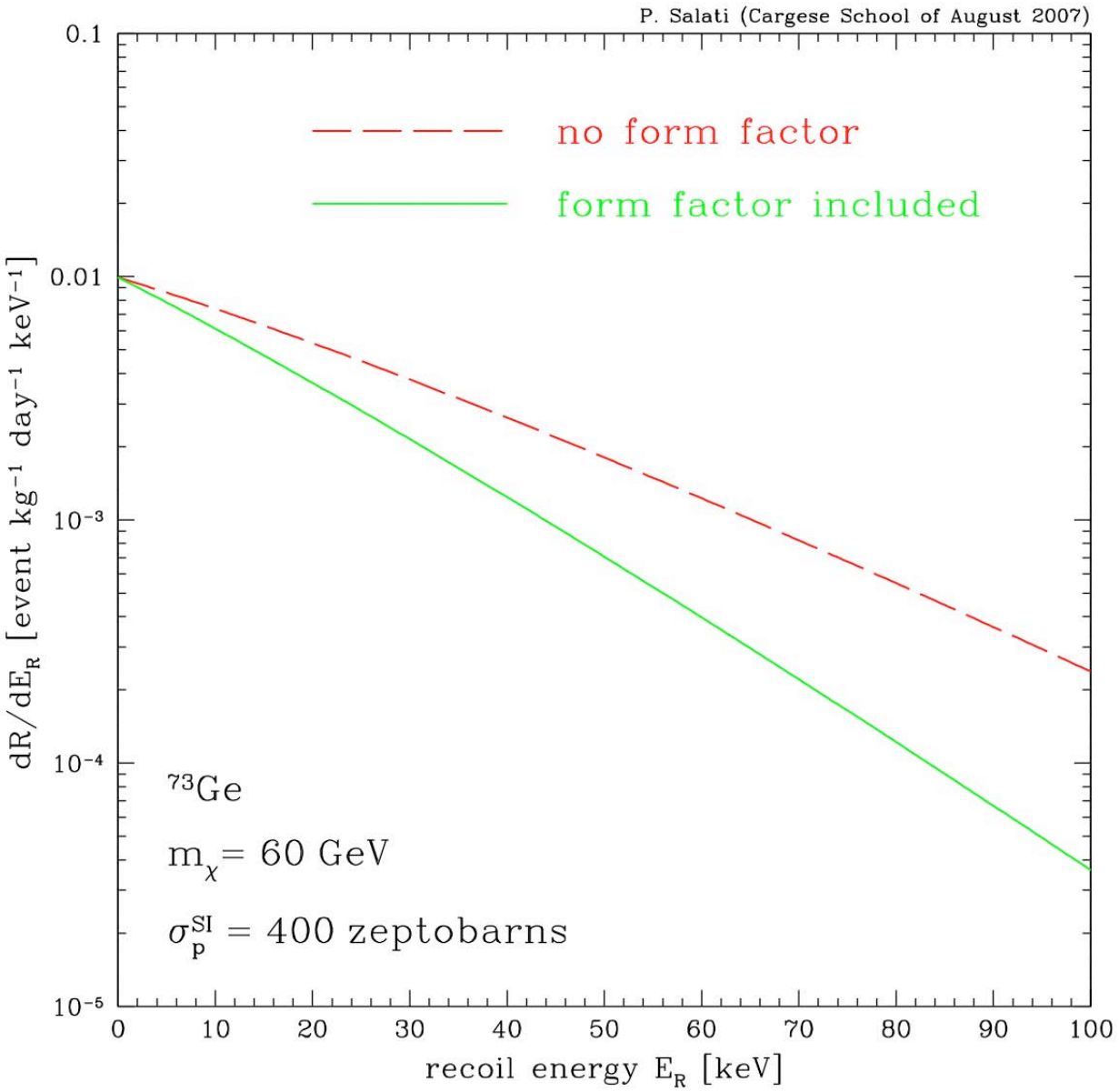
P. Salati (Cargese School of August 2007)
no form factor
form factor included
^{73}Ge
m_χ= 60 GeV
σ_p^{SI} = 400 zeptobarns
dR/dE$_R$ [event kg^{-1} day^{-1} keV^{-1}]
recoil energy E$_R$ [keV]
0.1
0.01
10^{-3}
10^{-4}
10^{-5}
0
10
20
30
40
50
60
70
80
90
100

Minimal Supersymmetric Standard Model

Focus Point:

- Decoupled sfermions, but RGE focusing makes weak scale natural
- LSP a heavy mixed bino-higgsino

Bulk:

- Light SUSY gives natural weak scale
- g-2 favored, but dangerous FCNC
- Light near-bino LSP

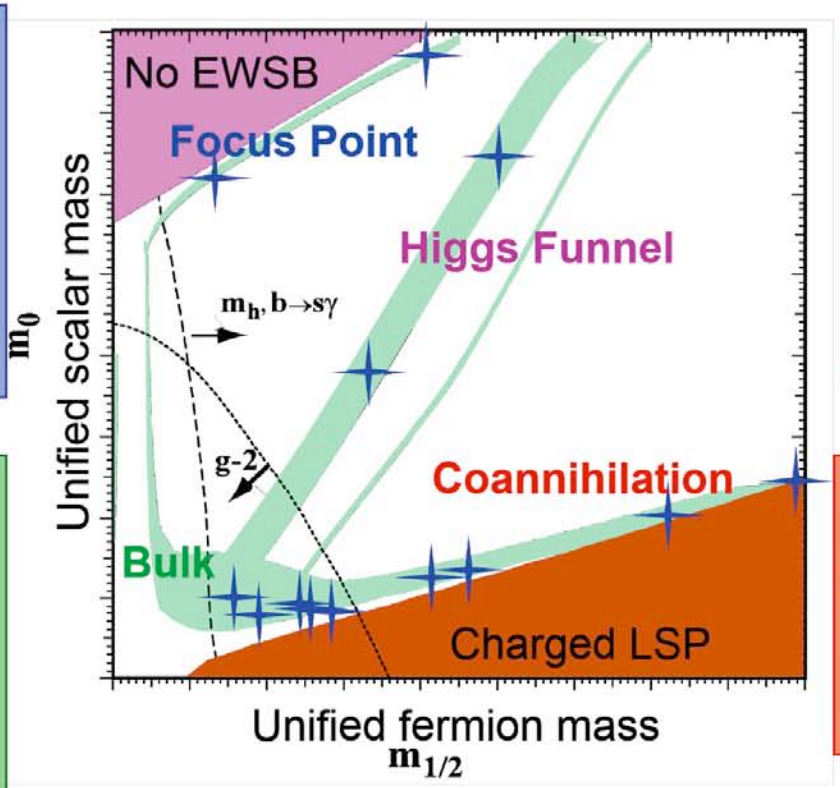

Battaglia et al., hep-ph/0112013

Higgs Funnel

- $M_A \sim 2M_\chi$ at large tan β, s-channel resonance speeds annihilation
- Heavy near-bino LSP

Coannihilation Tail

- LSP and NLSP nearly degenerate, allowing "cooperative" physics
- Heavy near-bino LSP

Lots of assumptions, but same basic mechanisms happen in larger SUSY spaces

Spin–Independent Interactions

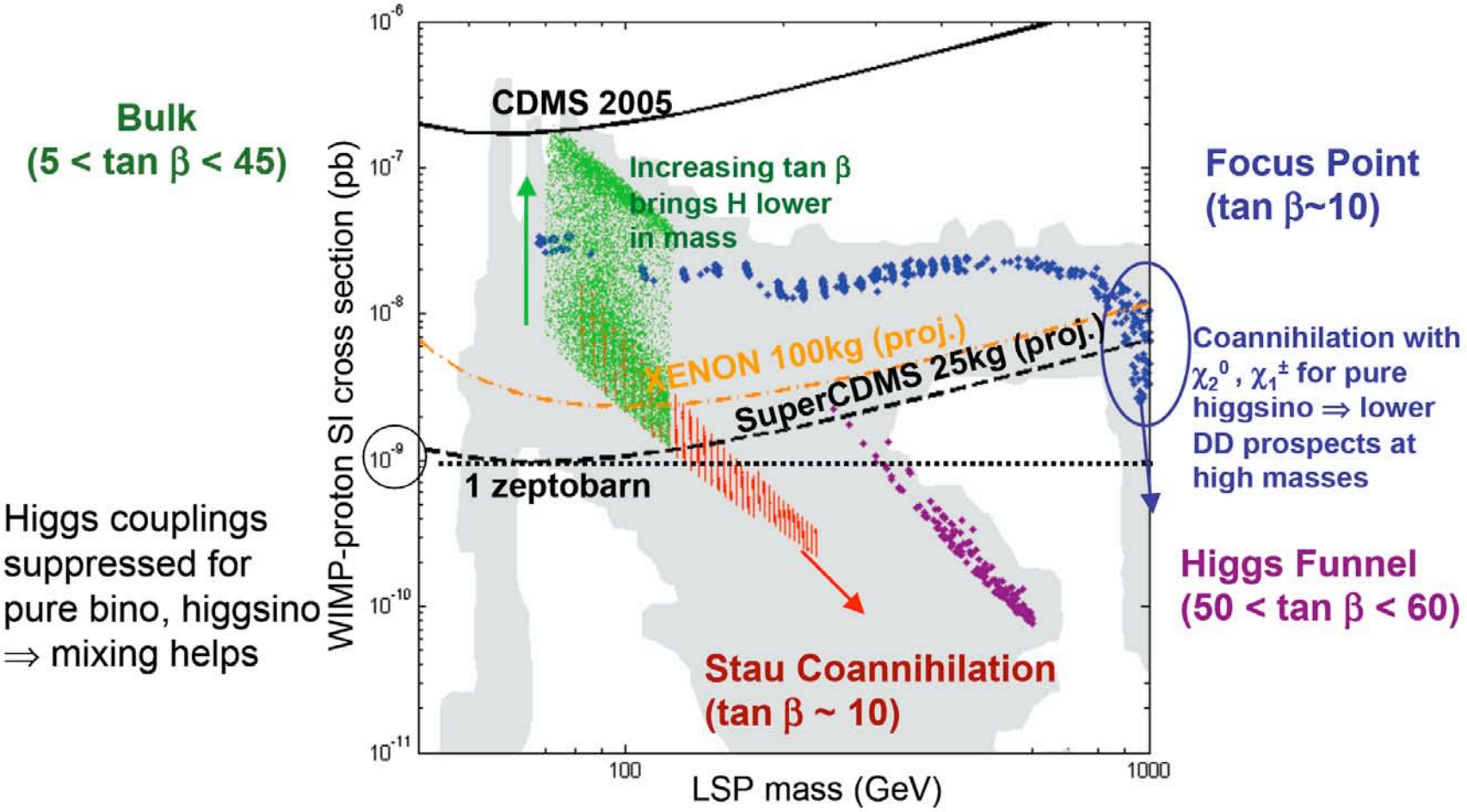

Parameter scans by JF and M. Battaglia using DarkSUSY 4.1; Shaded region Baltz & Gondolo mSUGRA (2004)

Spin–Dependent Interactions

Z-coupling sensitive to bino-higgsino mixings:

$$\sigma_{SD} \sim \left(|N_{13}|^2 - |N_{14}|^2\right)$$

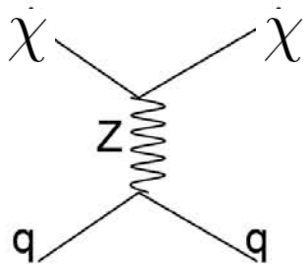

Similar structure, but poorer prospects for bulk region, more suppression at high masses in focus point

Same process for **indirect** detection using neutrinos from the sun

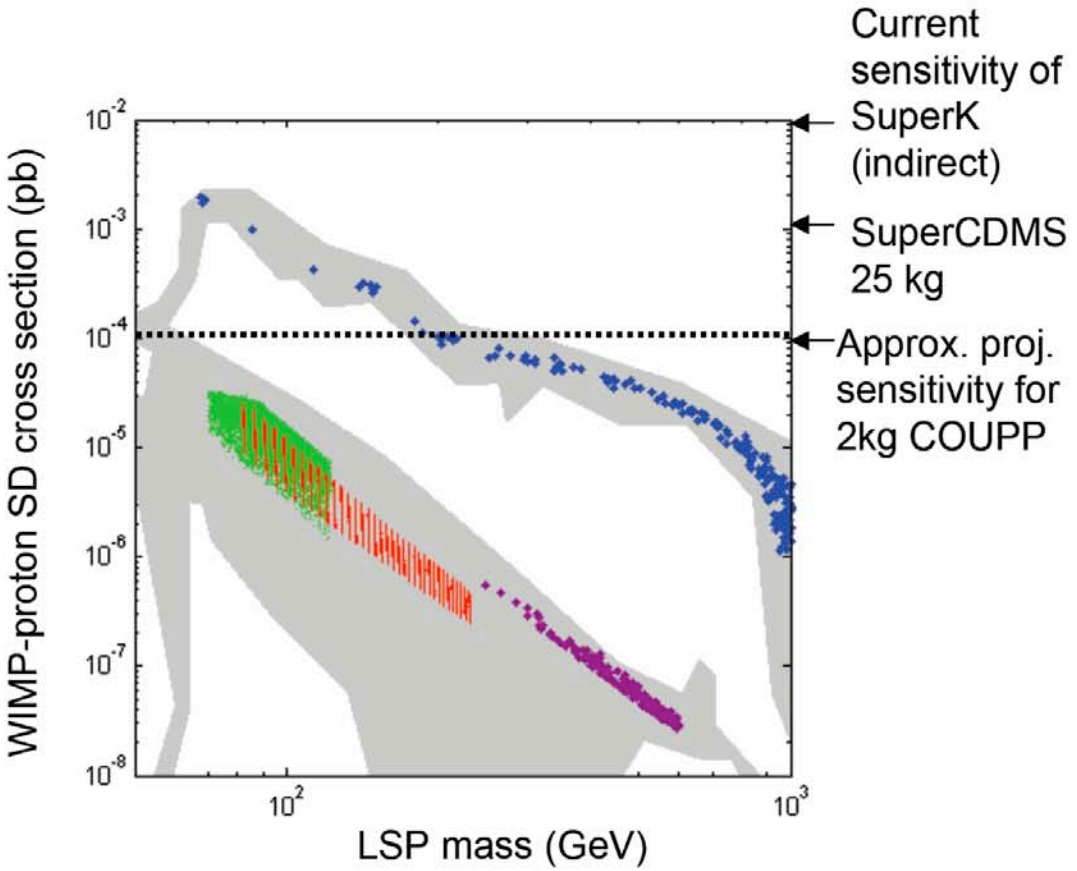

Parameter scans by JF and M. Battaglia using DarkSUSY 4.1; Shaded region Baltz & Gondolo mSUGRA (2004)

Direct Dark Matter Detection

Pierre Salati – Université de Savoie & **LAPTH**

1) Collision kinematics and the neutrino gas

2) Scattering rates, spectrum and nuclear corrections

3) The experimental endeavors and achievements

4) Future prospects

Cosmology and Particle Physics Beyond the Standard Models – Cargese – August 7, 2007

Summary of constraints

~ 1 keV $\leq E_R \leq \sim 100$ keV	$\Rightarrow$	very performant detector low threshold, good resolution
rate $\sim 0.01 - 0.1$ event kg^{-1} day^{-1}	$\Rightarrow$	large volume 100 kg to 1 ton
background $\rightarrow 0$	$\Rightarrow$	efficient shielding with high rejection level and discrimination

Background

Where does it come from ?		How to get rid of it ?
• cosmic rays and cosmic activation	$\Rightarrow$	underground laboratory
• natural radioactivity from rock (γ and neutrons)	$\Rightarrow$	passive and active shields
• natural radioactivity in materials	$\Rightarrow$	drastic material selection lead from sunken galleons
• radon in air from U–Th radioactive chains	$\Rightarrow$	antiradon facility
• radioactive dust	$\Rightarrow$	clean room
• irreducible background of γ & neutrons	$\Rightarrow$	**active background rejection :** **(i)** pulse shape discrimination **(ii)** quenching factor **(iii)** multiple neutron interactions **(iv)** annual modulation

Gran Sasso

http://www.lngs.infn.it/

- the largest underground laboratory
- located at 1 400 meters deep ~ 3800 mwe , on the vertical of Monte l'Aquila (2 600 meters high above sea level)
- in the Gran Sasso highway tunnel connecting L'Aquila to teramo about 120 km from Roma
- 3 main halls A, B and C of about 100x20x15m total volume 180 000 m^3
- muon flux reduction by a factor 10^6 : 24 μ/m^2/day
- permanent staff ~ 60 : physicists, technicians, engineers and administration staff

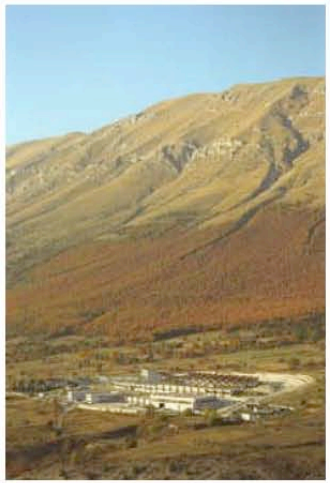

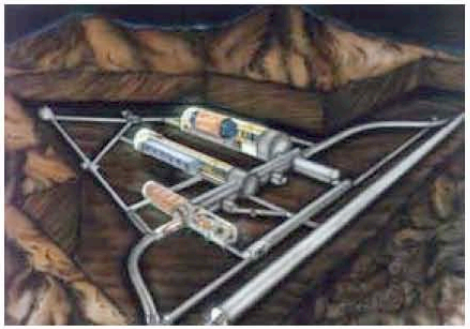

Soudan Underground Laboratory

http://www.hep.umn.edu/soudan/brochure.html

- Soudan Underground Mine State Park, Soudan, Minnesota
- depth : 710 m ~ 2100 mwe
- the lab currently hosts two large projects: MINOS CDMS II
- MINOS cavern is 95 m long, 15 m wide, and 13 m high.
- CDMS II cavern is similar in shape but only 70 meters long
- muon flux reduction by a factor 10^5

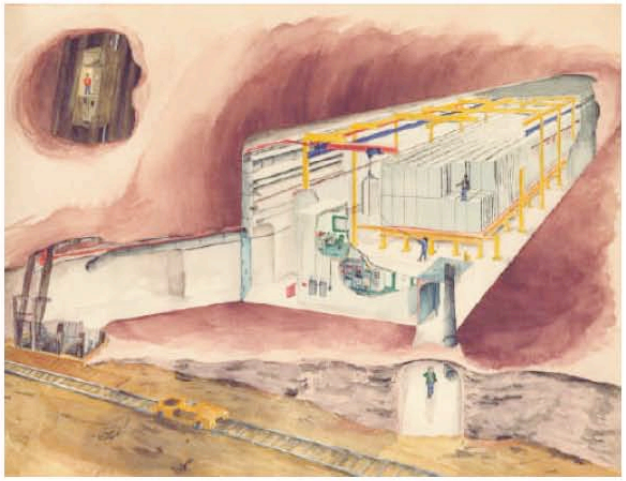

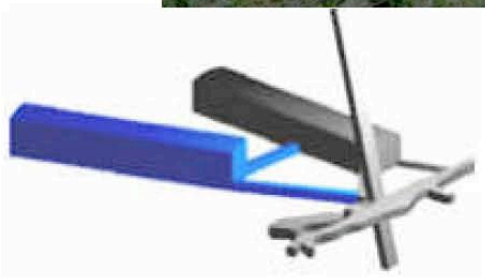

Radiation penetration

There is a great difference in the penetrating powers for alpha (α) particles, beta (b) particles, gamma (γ) rays or neutrons (n). Of the four types of radiation, alpha (α) particles are the easiest to stop. A sheet of paper is all that is needed for their absorption. However, it may require a material with a greater thickness and density to stop beta (β) particles. Gamma (γ) rays are stop by high Z materials. Neutrons have the most penetrating powers of the four radiation sources.

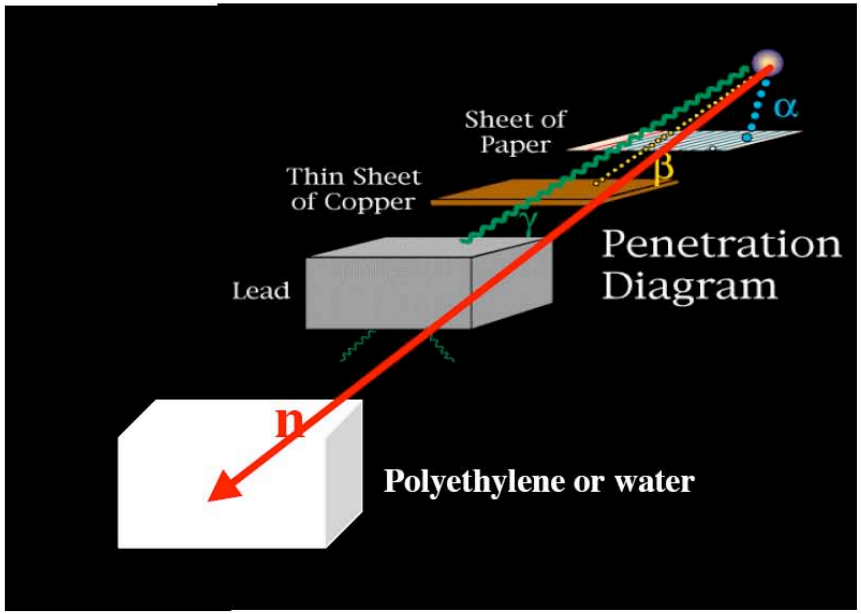

Underground radioactivity origins

Uranium and Thorium are naturally present in the rock of the cavity but also in all materials inside the lab. The U-Th desintegration produce γ and neutron backgrounds.
Energetic muon interactions with the rock components and materials in the lab produce high energy neutrons (few to tens MeV even GeV !)

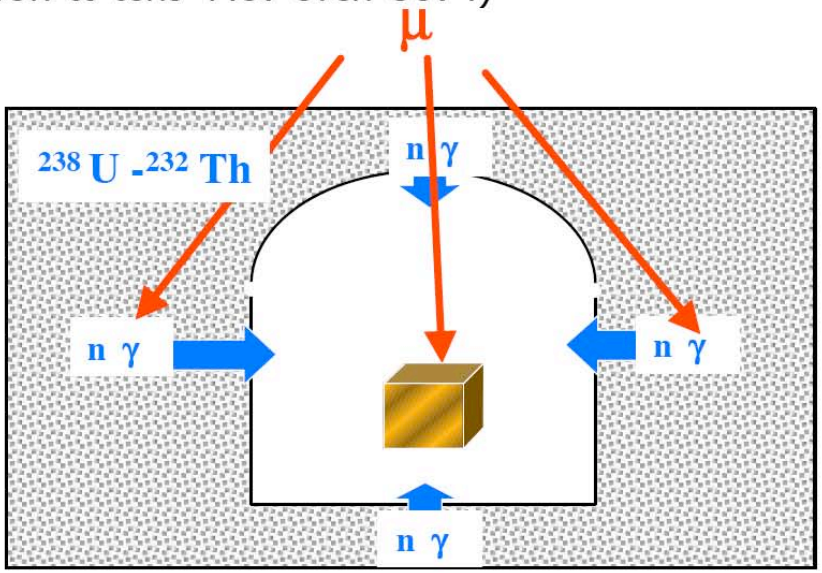

Nature of rocks → never homogeneous !
Large differences from one site to another one
Most of caverns are covered with concrete

The strategy used by several underground experiments sensitive to neutrons induced by muons is to use an active muon veto

Muons crossing the veto wrapping the experiment are tagged : data acquired in detectors during a muon crossing are subtracted

→ flux of neutrons from muons in Pb shield reduced

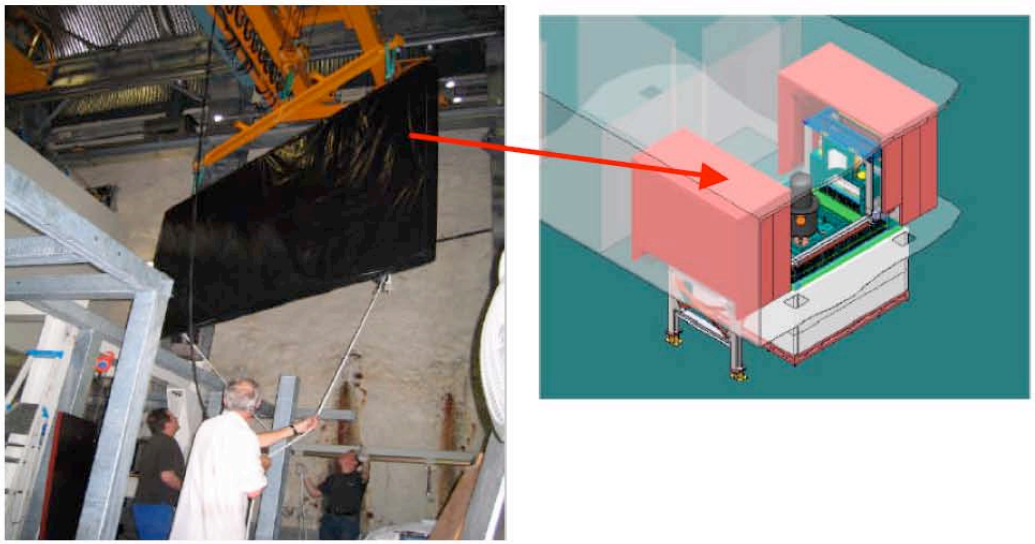

Multi-scattering neutrons

For energetic neutrons produced by muons in the rock the veto is not efficient but they can be identified by the multiple scattering interactions in an array of detectors.

Another possible identification is by using in the same array different targets (CDMS-II : Ge and Si, Ge is more sensitive to Wimps than Si).

EDW-II

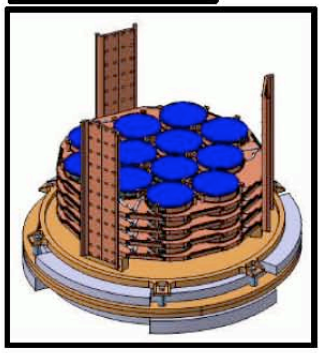

CUORE

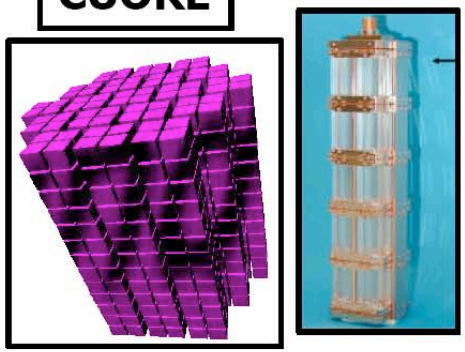

CDMS-II

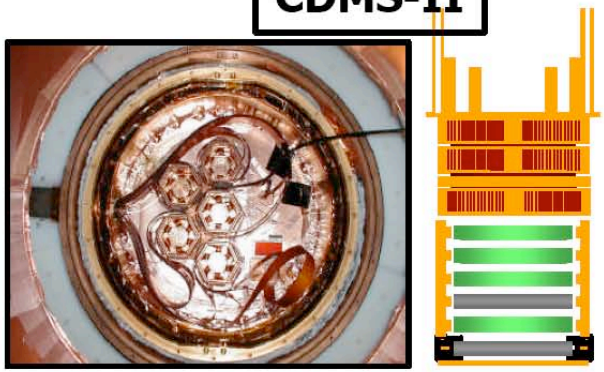

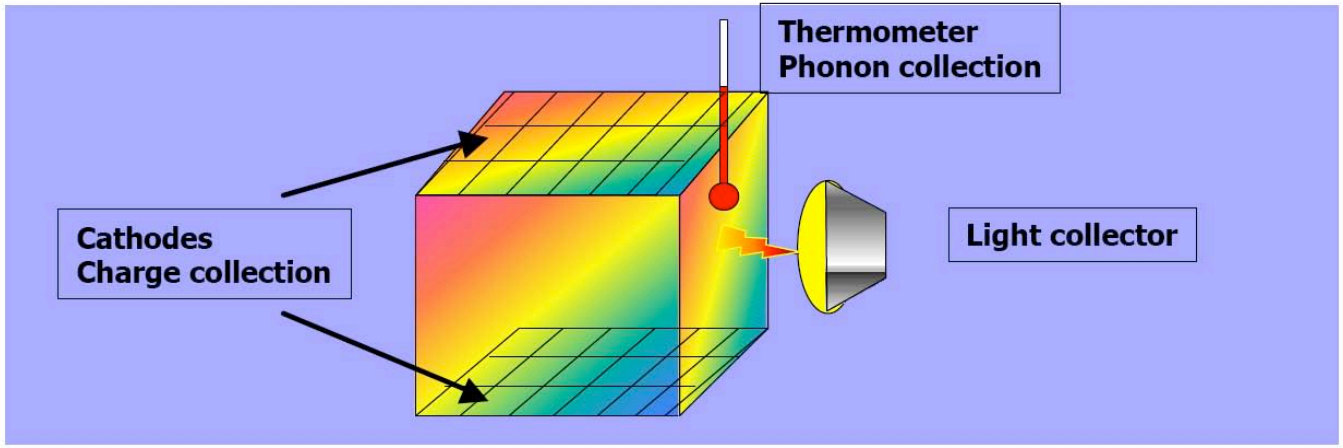

Xenon 10 as generic for ZEPLIN II ,WARP, ArDM

CDMS as generic for EDELWEISS & CRESST

Direct Detection Techniques

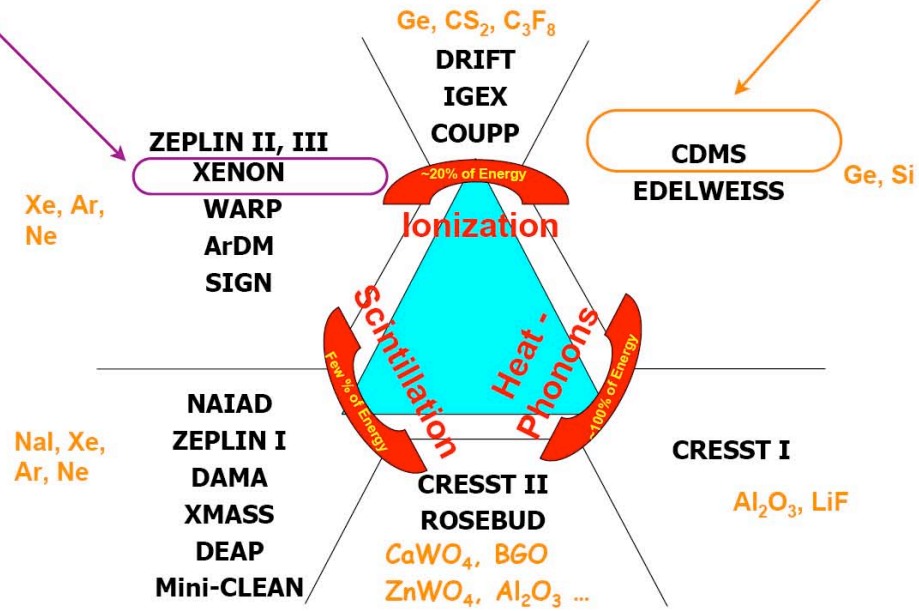

Active Background Rejection

Pulse Shape Discrimination

A nuclear recoil signal and a background e^- , γ event due to ambiant radioactivity will exhibit different pulse shapes.

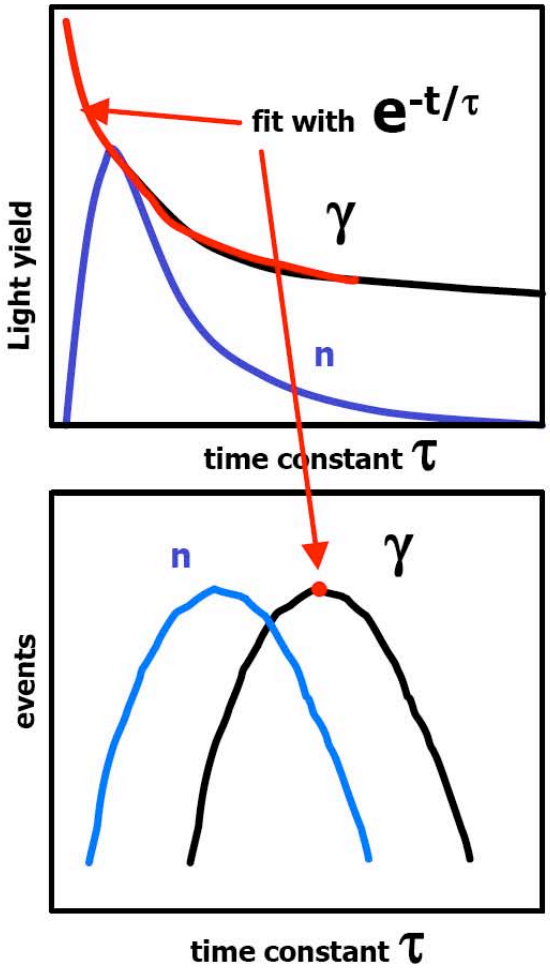

statistical rejection method

Method commonly used with scintillators NaI, CsI, Xe, …

Quenching Factor

Upon the nature of the detector target material we will have a heat signal but also a charge or light signal. Nuclear recoils produce less ionization or light relative to electron recoils from e^--γ background ; whereas they will produce the same heat.
In order to compare the calculated rates with the measured ones, the differential rate dR/dE_R is expressed as a function of the electron–equivalent energy E_{ee} .
The quantity E_{ee} is simply proportional to the nuclear recoil energy through the quenching factor Q:

Quenching Factor: $Q= E_{ee}/E_R$

<u>event-by-event rejection method</u>

Method commonly used with combined technologies :
calorimeters + semiconductor/scintillator
Ge, Si, $CaWO_4$, Al_2O_3, …

Liquid Xenon : ionization + scintillation

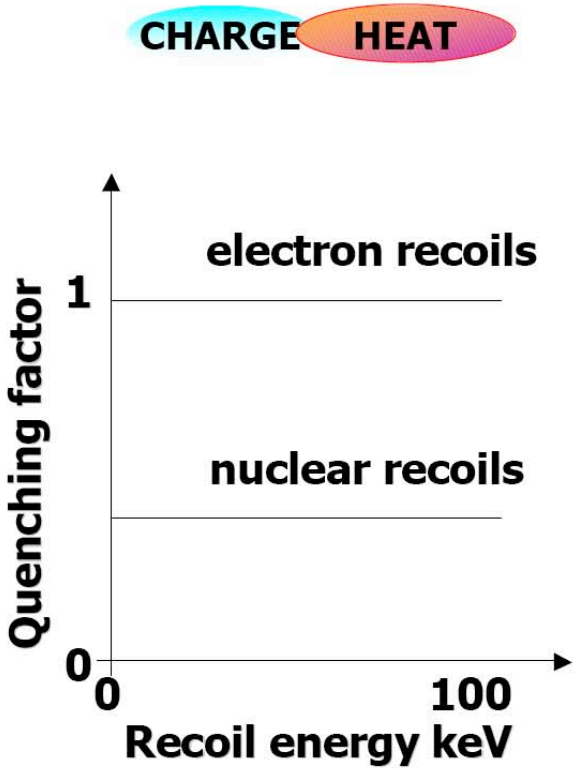
CHARGE
HEAT
Quenching factor
1
0
electron recoils
nuclear recoils
0
100
Recoil energy keV

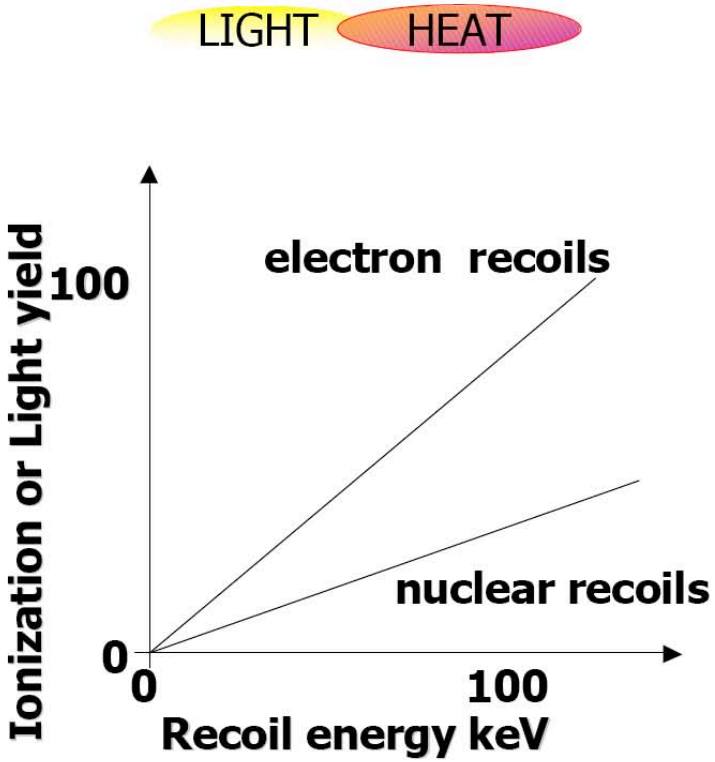
LIGHT
HEAT
Ionization or Light yield
100
0
electron recoils
nuclear recoils
0
100
Recoil energy keV

CDMS

http://cdms.berkeley.edu/

CDMS is the first experiment to develop the simultaneous measurement of heat and ionization signals in 1993

Since 2002 the second phase of the experiment is installed in the Soudan mine (depth: 713 m (2090 mwe))

Towers of 6 detectors : Ge (250g) and Si (100g) with Superconducting thin films of W, Al for an active background rejection

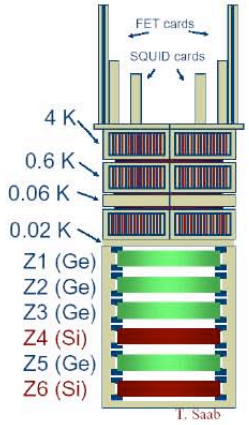

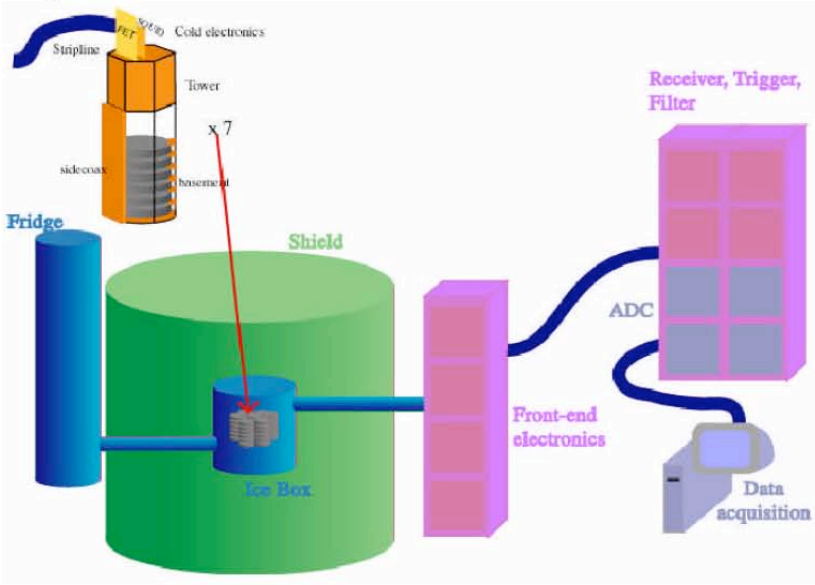

CDMS-II

Background rejection evaluated with external sources :

- **^{133}Ba γ source**
- **^{252}Cf neutron source**

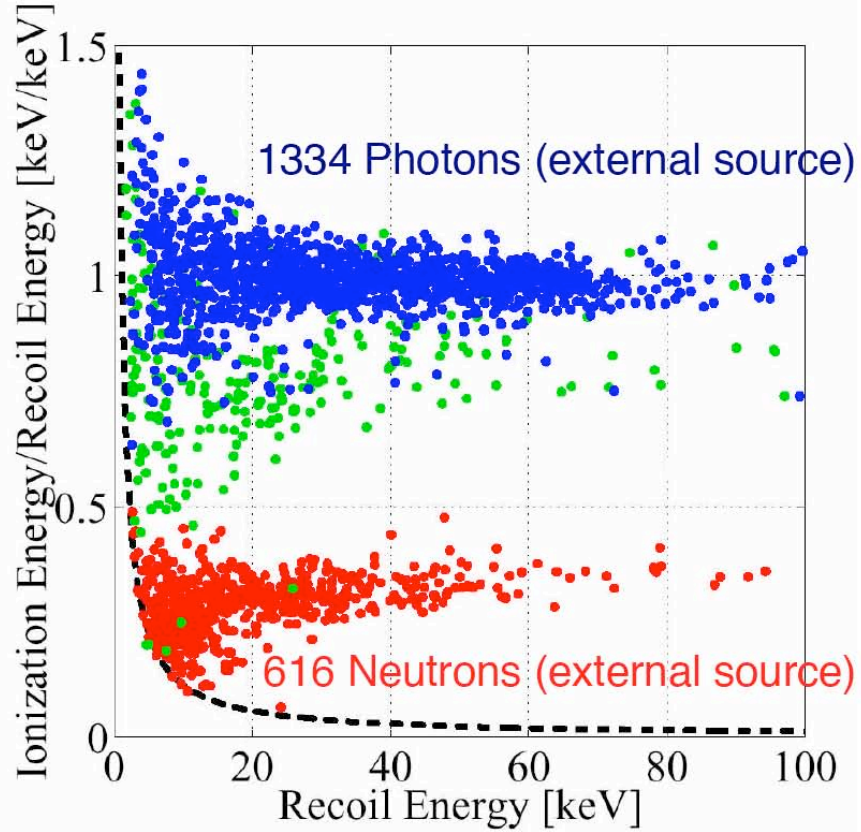

Surface events in heat-ionization cryogenic detectors

Electron recoils near detector surface result in reduced ionization yield inducing a lower Q value than expected and give rise to a pollution in the nuclear recoil zone.

CDMS

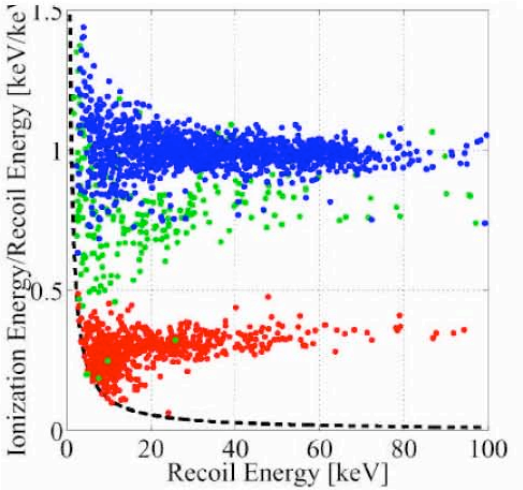

Edelweiss

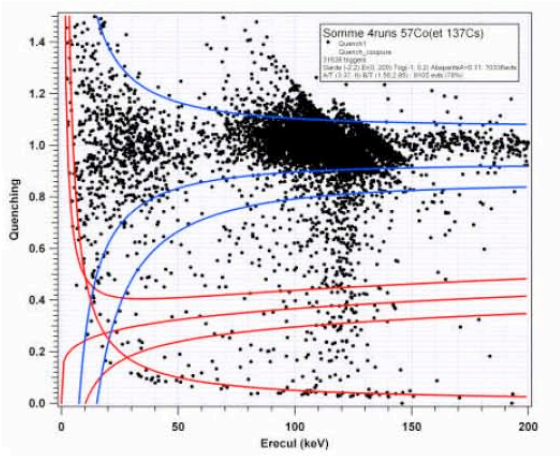

^{57}Co calibration run

→ *New detector developments for the detection of non-equilibrium phonons:*

1. **thin film sensors in the metal insulator transition : EDELWEISS-II**
2. **transition edge sensors : thermometers based on the superconducting-normal transition : CDMS-II**

Both technologies are able to localize the interaction allowing the rejection of surface events

Surface events in CDMS-II

ZIP detectors : **Z-sensitive Ionization-Phonon sensor**

Athermal phonons are trapped in aluminium thin films coupled to tungsten sensors. Signal risetime and delay give information about the 3D position of the event, in particular the proximity to the surface

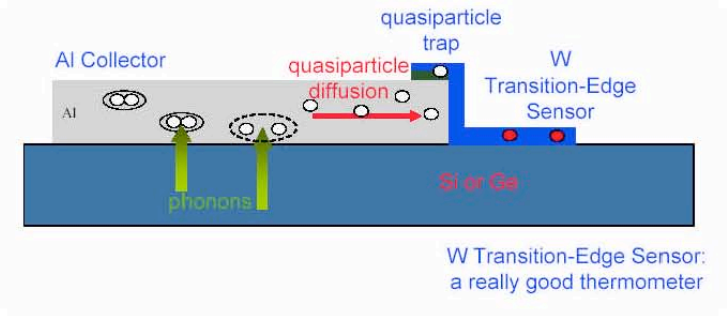

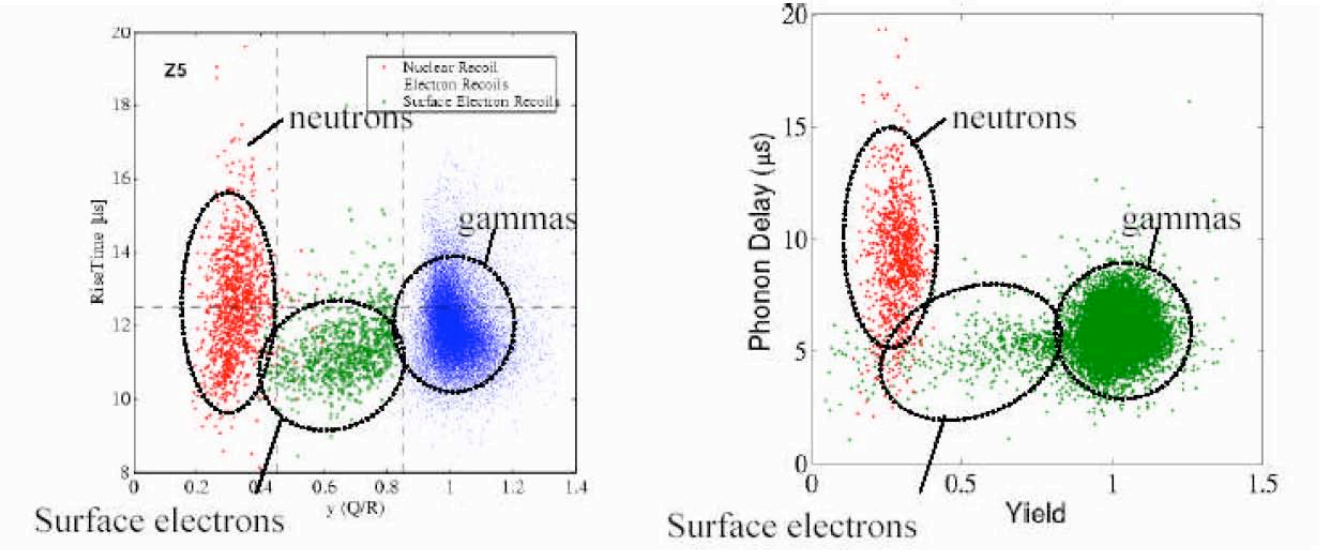

WIMP-search data

Prior to timing cuts

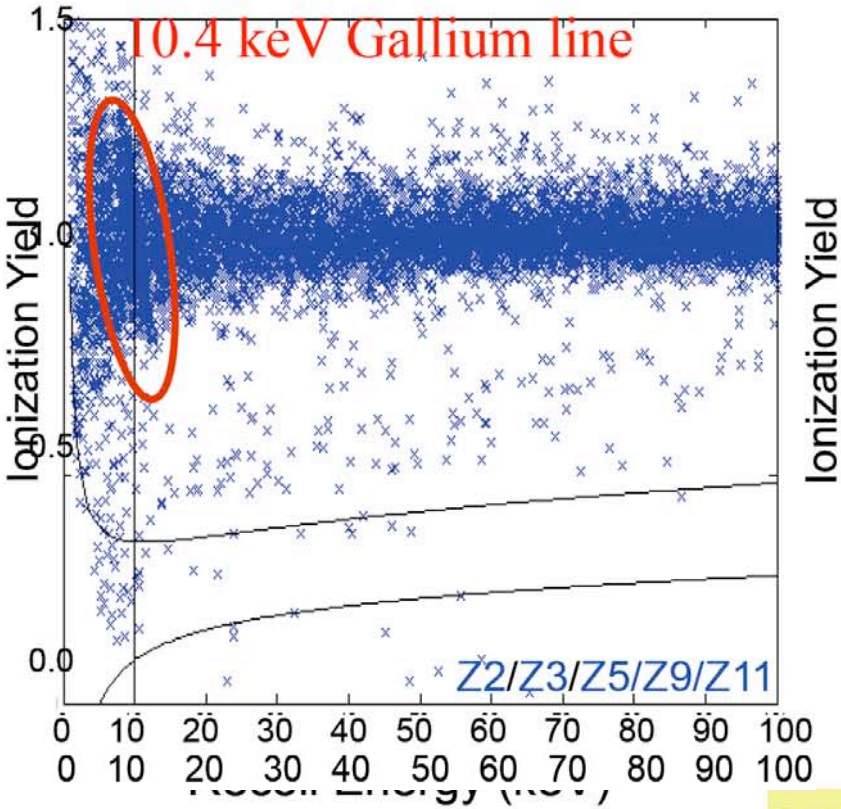

90 kg.days

34kg.days after cuts

After timing cuts, which reject most electron recoils

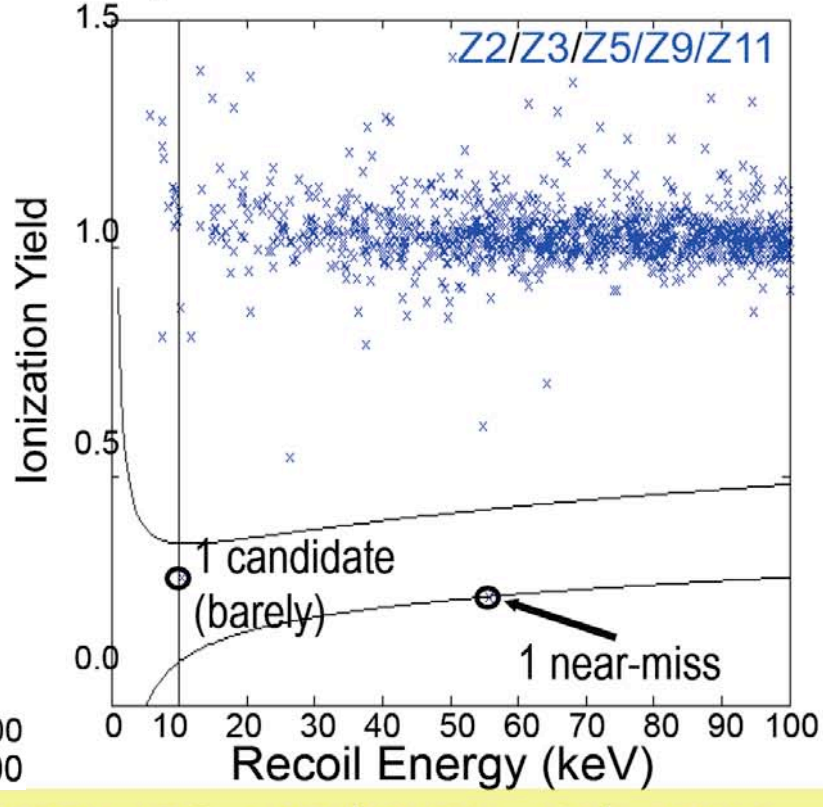

ESTIMATE: 0.37 ±0.15(stat.) ± 0.20(sys.) electron recoils,
0.05 recoils from neutrons expected

Limit or Discovery ?

- The expected number of events $n_{\rm theo}$ depends on the total cross section

$$\sigma_{\rm N} = \sigma_{\rm N}^{\rm SI} + \sigma_{\rm N}^{\rm SD}$$

After rejection of the background, a number $n_{\rm obs}$ of events still pass the various cuts

$$n_{\rm obs} = n_{\rm back} + n_{\rm WIMP}$$

- An enormous number N of DM particles have crossed the detector during the observation run. Each of these species has a vanishingly small probability p to interact with a nucleus. In the limit where N goes to infinity **at constant** $a = p \times N$, Poisson statistics applies – I leave you this as an additional exercise – and the probability to detect n particles is given by

$$P\left\{n|a\right\} = \frac{a^n}{n!}\, e^{-a}$$

- So far, the remaining events $n_{\rm obs}$ have been interpreted as **background** so that $n_{\rm WIMP}$ is compatible with 0. A conservative limit is set on the cross section with a confidence level C.L. by requiring that

$$P\left\{n_{\rm obs}|n_{\rm theo}\right\} \leq (1 - {\rm C.L.})$$

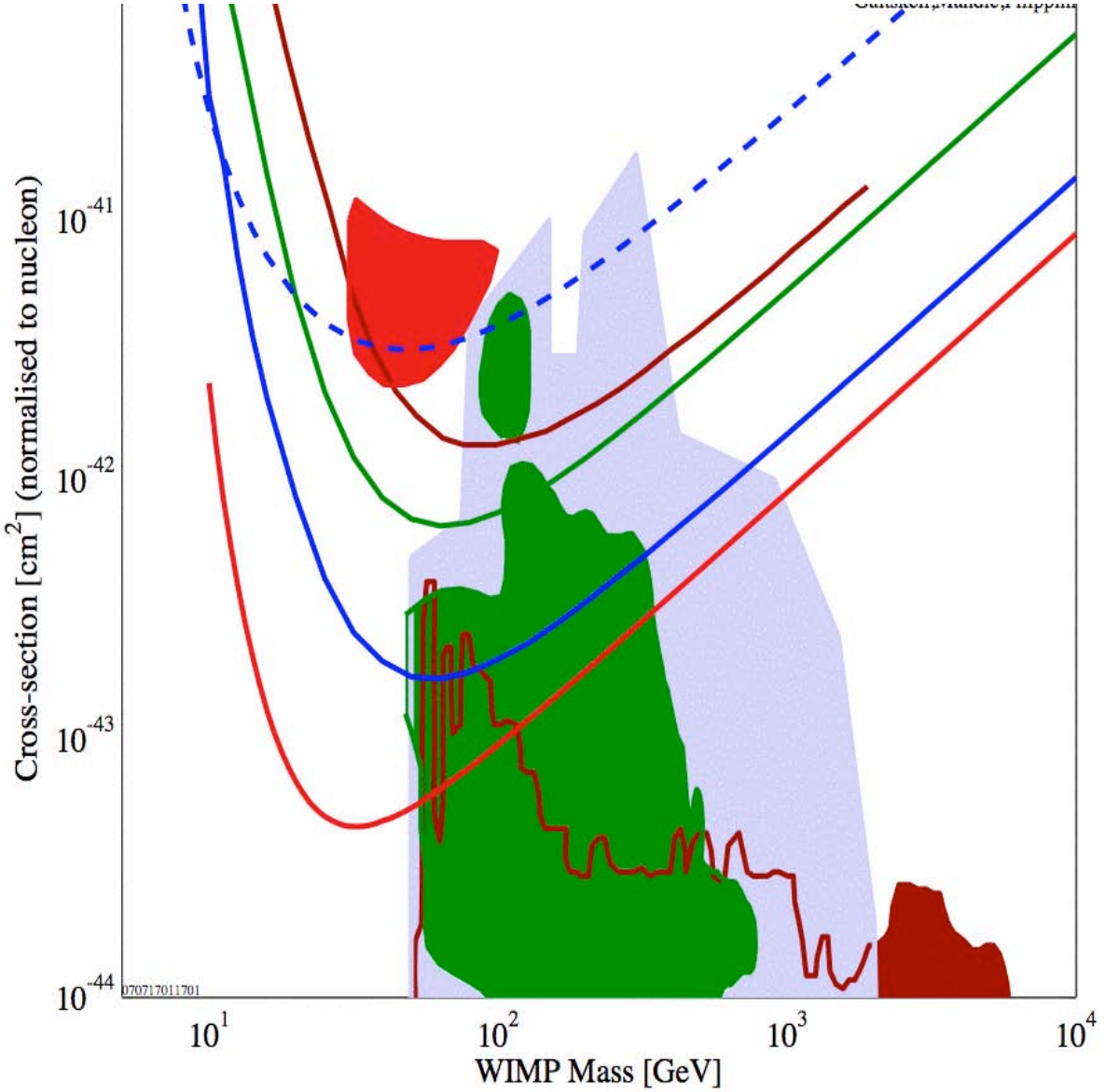

DATA listed top to bottom on plot
CDMS (Soudan) 2005 Si (7 keV threshold)
DAMA 2000 58k kg-days NaI Ann.Mod. 3sigma,w/o DAMA 1996 limit
Edelweiss I final limit, 62 kg-days Ge 2000+2002+2003 limit
ZEPLIN II (Jan 2007) result
CDMS (Soudan) 2004 + 2005 Ge (7 keV threshold)
XENON10 2007 (Net 136 kg-d)
Ruiz de Austri/Trotta/Roszkowski 2007, CMSSM Markov Chain Monte Carlos (1
Baltz and Gondolo 2003
Baltz and Gondolo, 2004, Markov Chain Monte Carlos
070717011701

Xenon 10

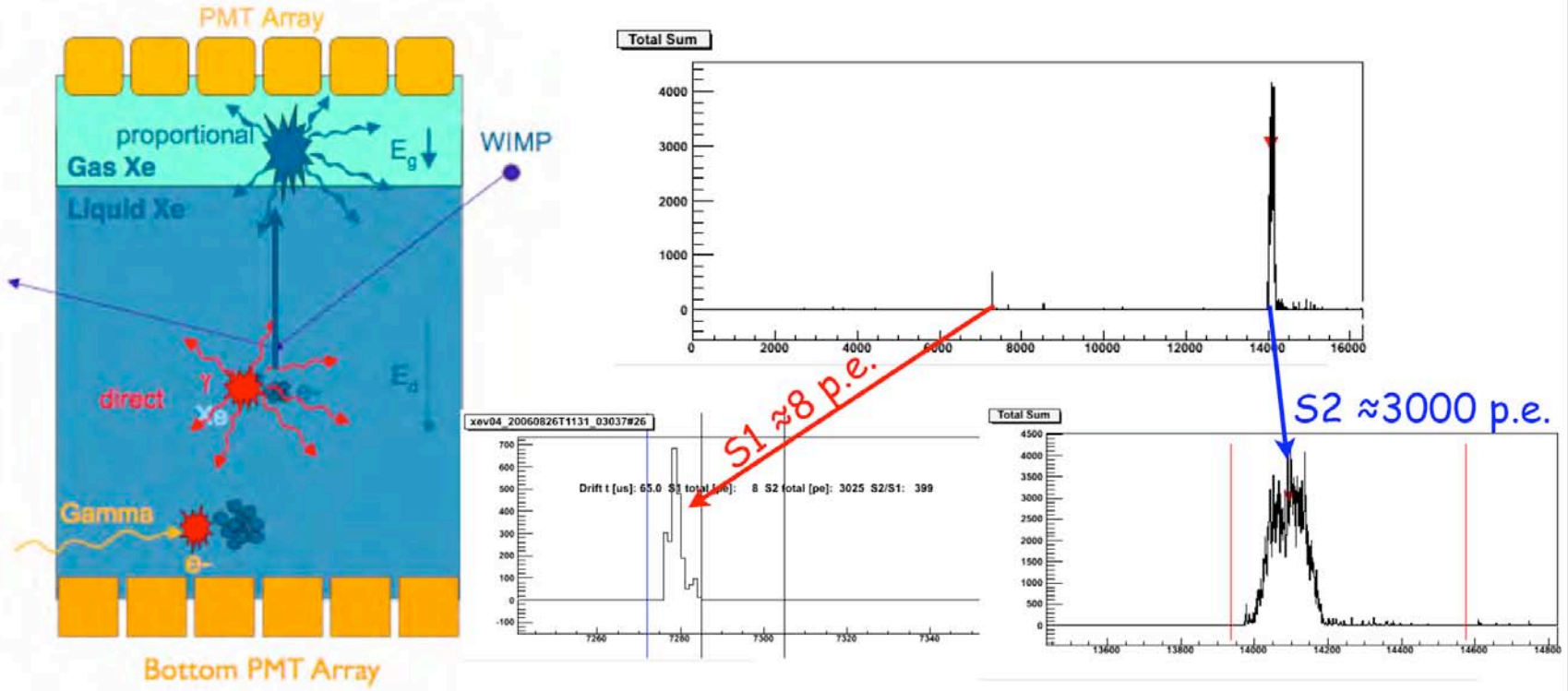

Liquid Xenon: Scintillation + ionization

two photon pulses => depth

Breakthrough: extraction of electrons from liquid

importance of having detector at the bottom

Xenon 10

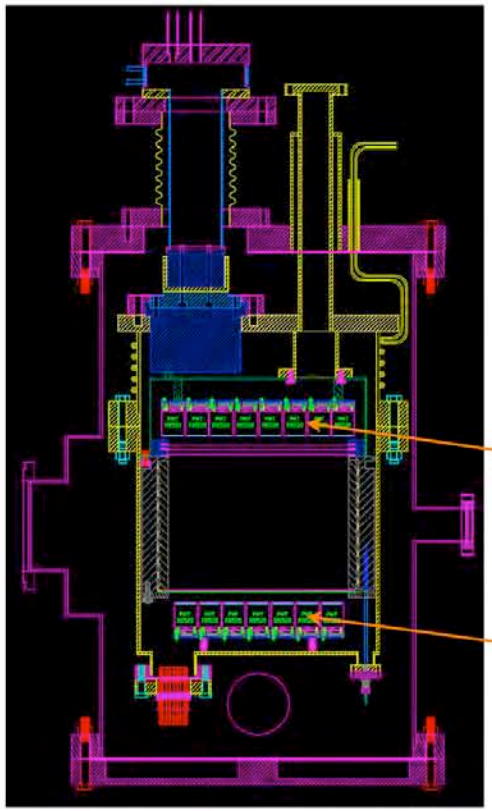

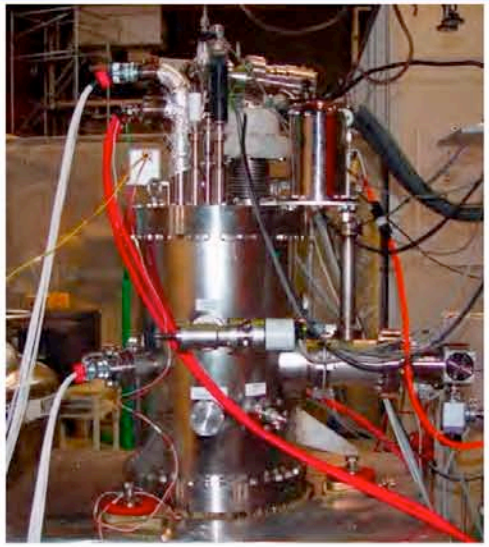

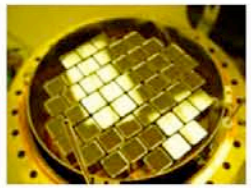

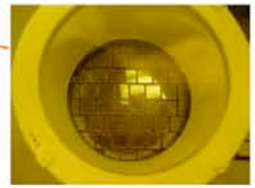

First Results from the XENON10 Dark Matter Experiment at the Gran Sasso National Laboratory

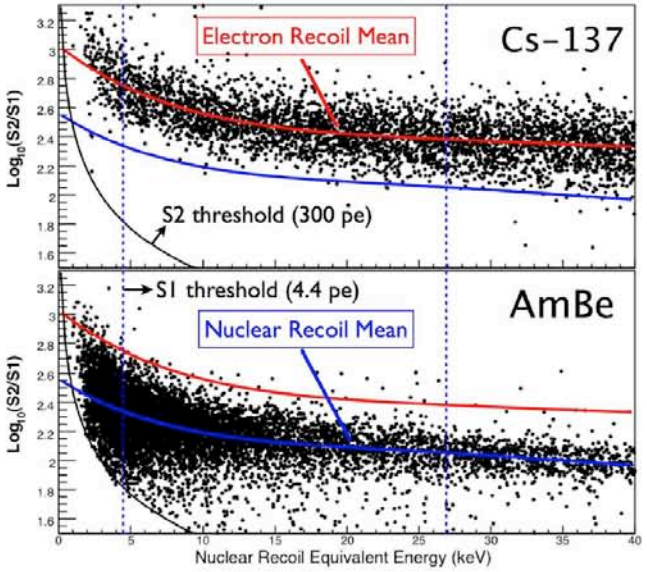

FIG. 1: $\mathrm{Log}_{10}(S2/S1)$ as a function of energy for electron recoils (top) and nuclear recoils (bottom) from calibration data. The colored lines are the mean $\mathrm{Log}_{10}(S2/S1)$ values of the electron recoil (upper, red) and nuclear recoil (lower, blue) bands. The region between the two vertical dashed lines is the energy window (4.5 - 26.9 keV nuclear recoil equivalent energy) chosen for the WIMP search. An $S2$ software threshold of 300 pe is also imposed (black lines).

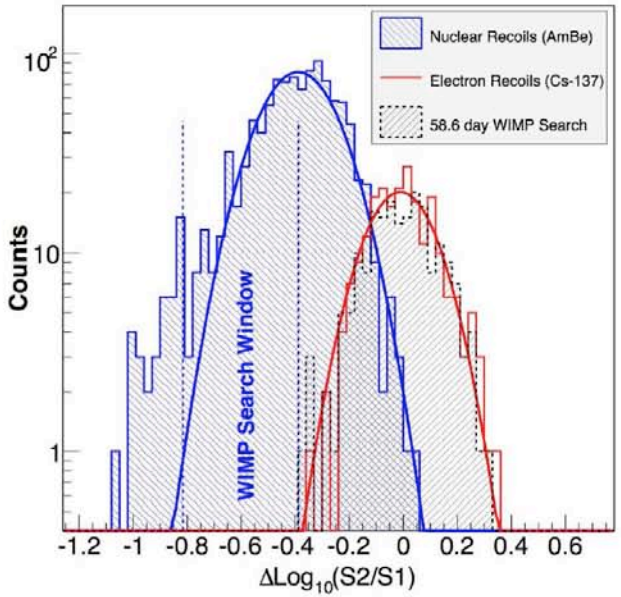

FIG. 2: Distributions of $\Delta\mathrm{Log}_{10}(S2/S1)$ for nuclear recoils, electron recoils and WIMP search data for one energy bin (6.7-9.0 keV nuclear recoil equivalent energy). The nuclear recoil acceptance (WIMP Search Window) is defined by the two vertical lines, which are the -3σ and mean from a Gaussian fit to the nuclear recoil $\Delta\mathrm{Log}_{10}(S2/S1)$ distribution. The $\Delta\mathrm{Log}_{10}(S2/S1)$ distribution from electron recoils is fit by a Gaussian function. The fit parameters are used to predict the number of statistical leakage events (see Table I).

First Results from the XENON10 Dark Matter Experiment at the Gran Sasso National Laboratory

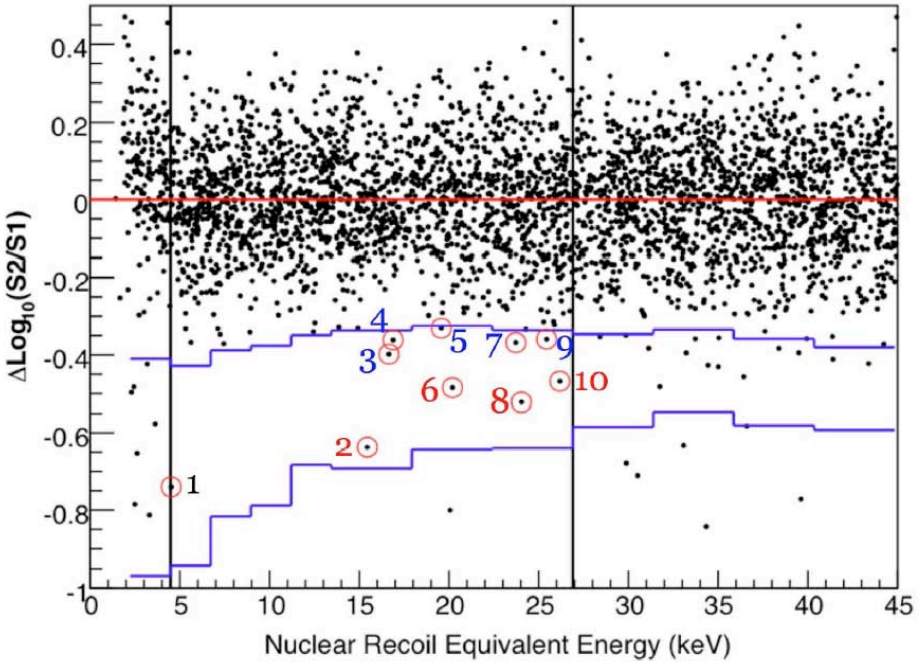

FIG. 4: Results from 58.6 live-days of WIMP-search in the 5.4 kg LXe target. The WIMP search window was defined between the two vertical lines (4.5 to 26.9 keV nuclear recoil equivalent energy) and blue lines (about 50% nuclear recoil acceptance).

First Results from the XENON10 Dark Matter Experiment at the Gran Sasso National Laboratory

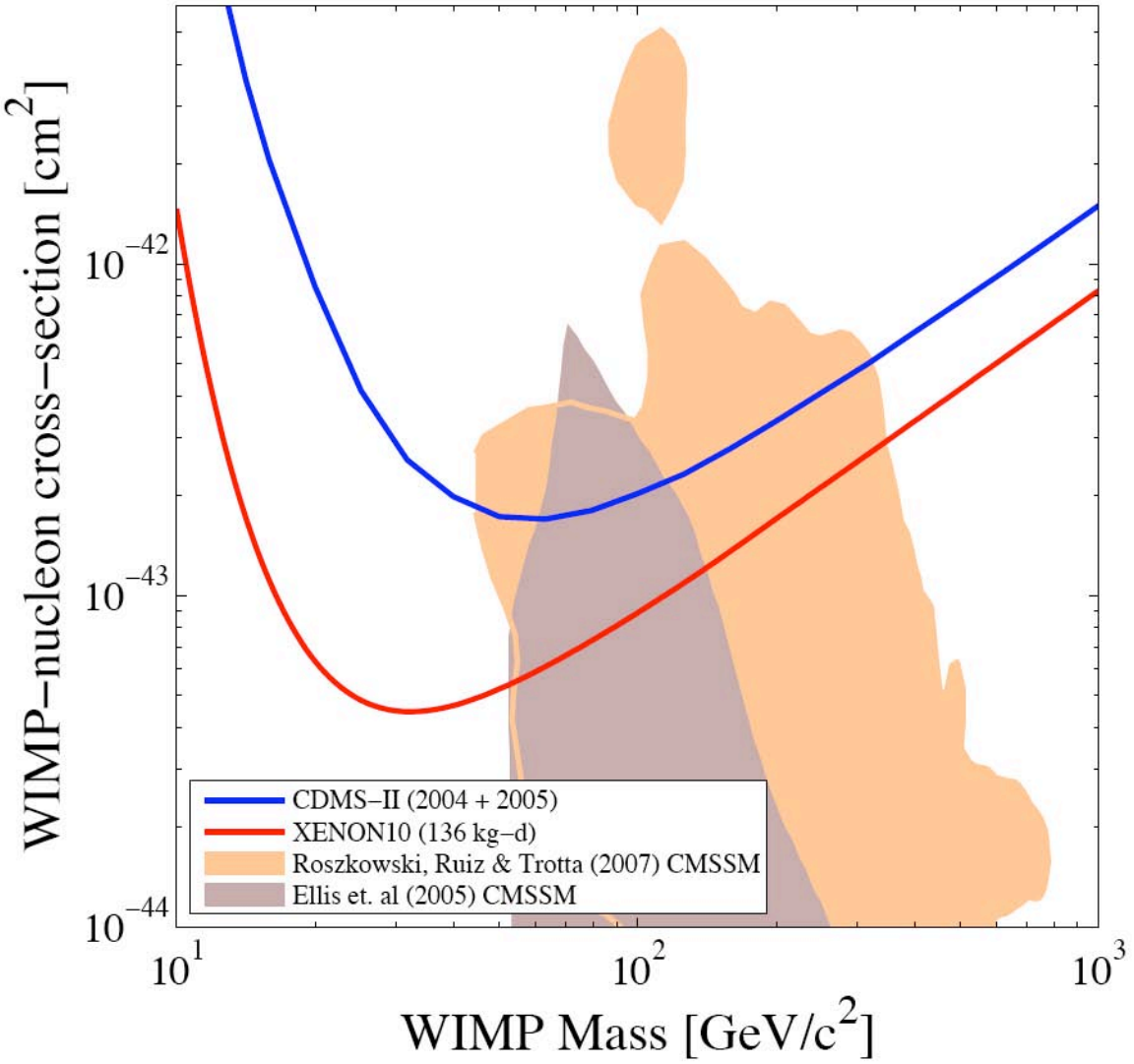

arXiv:0706.0039v1 [astro-ph] 31 May 2007

Direct Dark Matter Detection

Pierre Salati – Université de Savoie & **LAPTH**

1) Collision kinematics and the nucleus recoil

2) Scattering rates, motion and nucleon content

3) The experimental milestones and achievements

4) Future prospects

Limit or Discovery ?

- The expected number of events $n_{\rm theo}$ depends on the total cross section

$$\sigma_{\rm N} = \sigma_{\rm N}^{\rm SI} + \sigma_{\rm N}^{\rm SD}$$

After rejection of the background, a number $n_{\rm obs}$ of events still pass the various cuts

$$n_{\rm obs} = n_{\rm back} + n_{\rm WIMP}$$

- So far, the remaining events $n_{\rm obs}$ have been interpreted as **background** so that $n_{\rm WIMP}$ is compatible with 0. A conservative limit is set on the cross section with a confidence level C.L. by requiring that

$$P\left\{n_{\rm obs}|n_{\rm theo}\right\} \leq (1 - {\rm C.L.})$$

In the case of CDMS II, $n_{\rm obs} \sim 0$. Requiring that $P\left\{0|n_{\rm theo}\right\} \leq 10\%$ translates into excluding cross sections for which $n_{\rm theo} \geq \ln(10)$ at the 90% confidence level

- If the background is **perfectly** rejected, the cross section is measured from

$$n_{\rm theo}\left(\sigma_{\rm N}\right) \equiv n_{\rm WIMP}$$

Velocity distribution corrected for the Earth motion

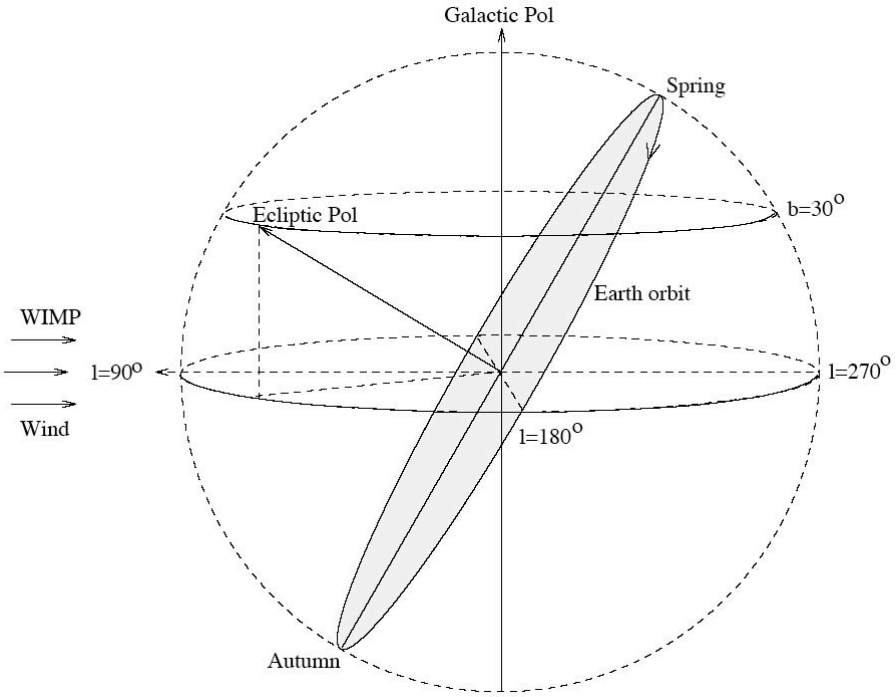

• The Earth moves actually in the Galactic frame and its velocity is of the same order of magnitude as V_C

$$v_e = V_C \cdot \left\{ 1.05 \; + \; 0.07 \cos \left\{ \frac{2\pi (t - t_P)}{1 \text{ yr}} \right\} \right\}$$

where t_P is June 2nd $\pm$ 1.3 days.

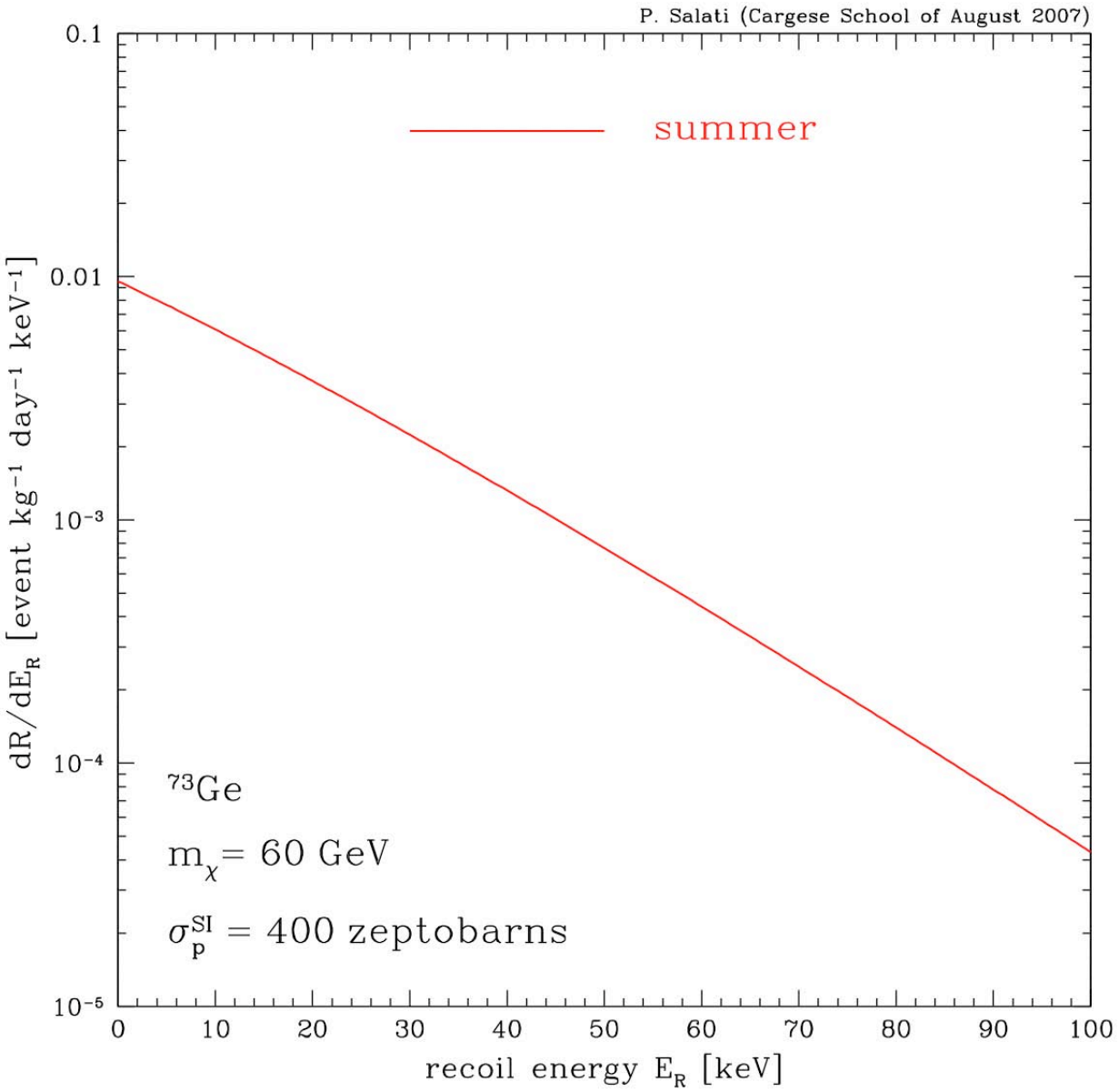
P. Salati (Cargese School of August 2007)
summer
^{73}Ge
m_χ= 60 GeV
σ_p^{SI} = 400 zeptobarns
dR/dE$_R$ [event kg^{-1} day^{-1} keV^{-1}]
recoil energy E$_R$ [keV]
0.1
0.01
10^{-3}
10^{-4}
10^{-5}
0
10
20
30
40
50
60
70
80
90
100

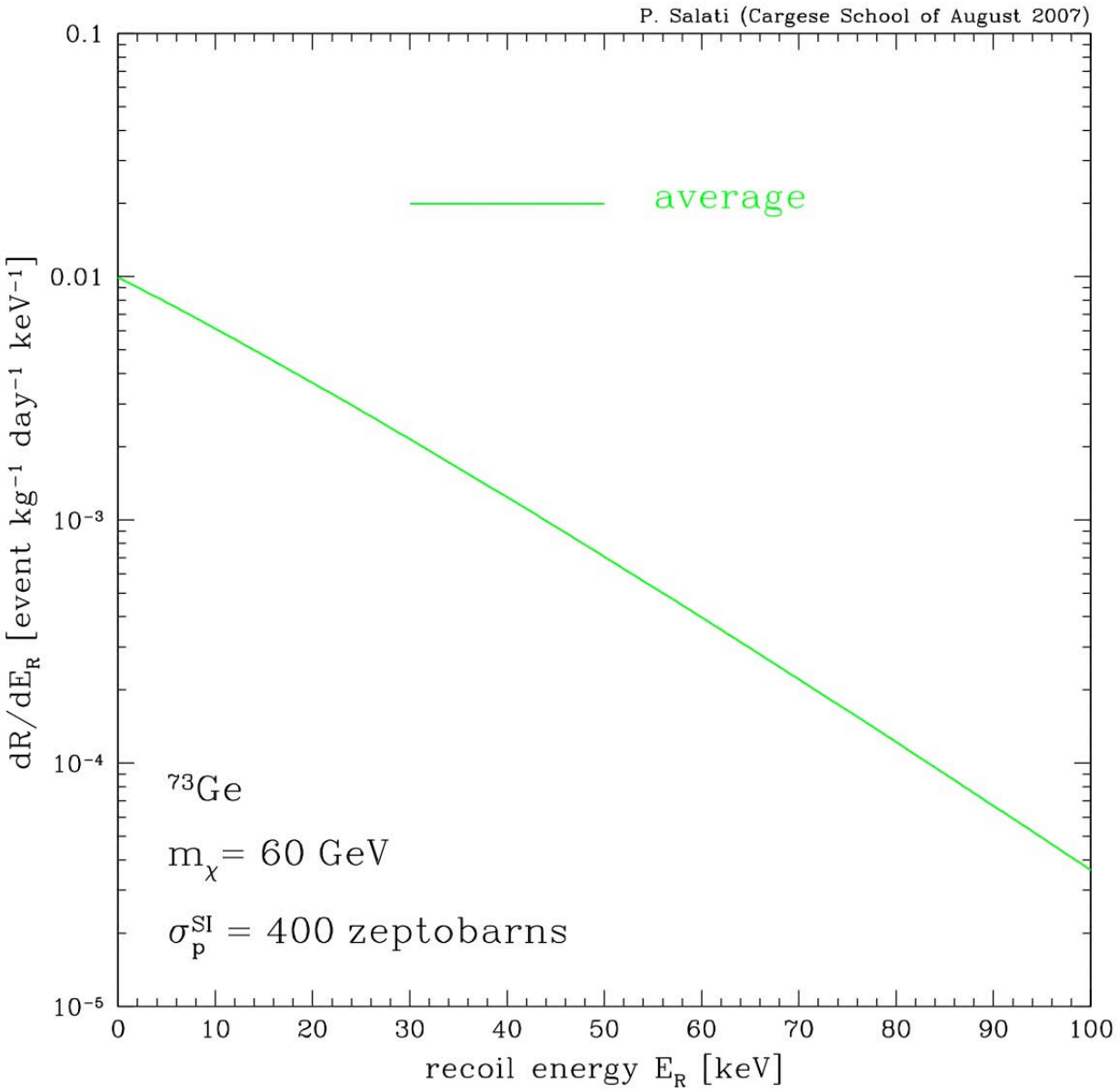
P. Salati (Cargese School of August 2007)
average
^{73}Ge
m_χ= 60 GeV
σ_p^{SI} = 400 zeptobarns
dR/dE$_R$ [event kg^{-1} day^{-1} keV^{-1}]
recoil energy E$_R$ [keV]
0.1
0.01
10^{-3}
10^{-4}
10^{-5}
0
10
20
30
40
50
60
70
80
90
100

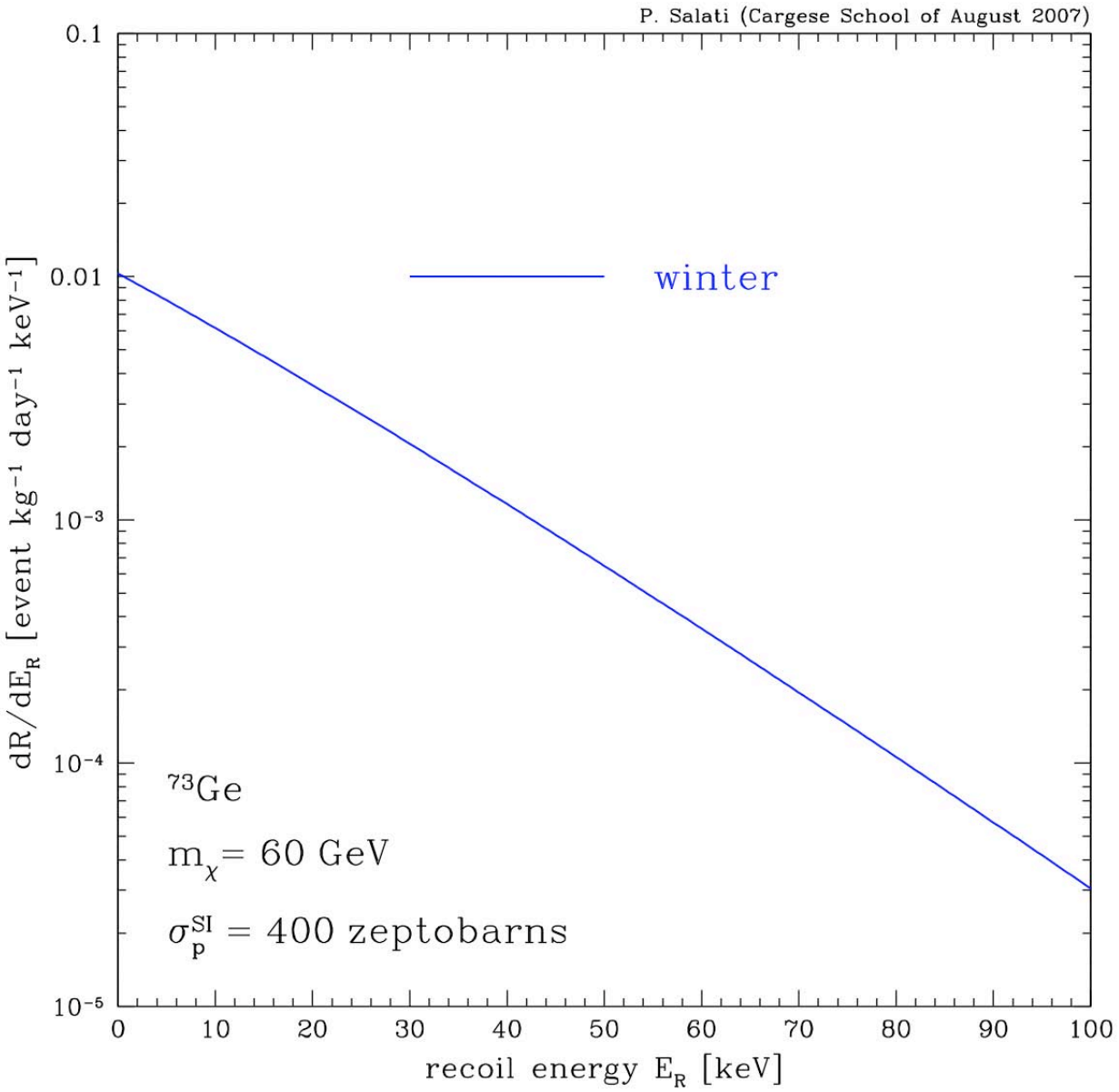
P. Salati (Cargese School of August 2007)
0.1
0.01
10^{-3}
10^{-4}
10^{-5}
dR/dE_R [event kg^{-1} day^{-1} keV^{-1}]
winter
^{73}Ge
m_χ= 60 GeV
σ_p^{SI} = 400 zeptobarns
0
10
20
30
40
50
60
70
80
90
100
recoil energy E_R [keV]

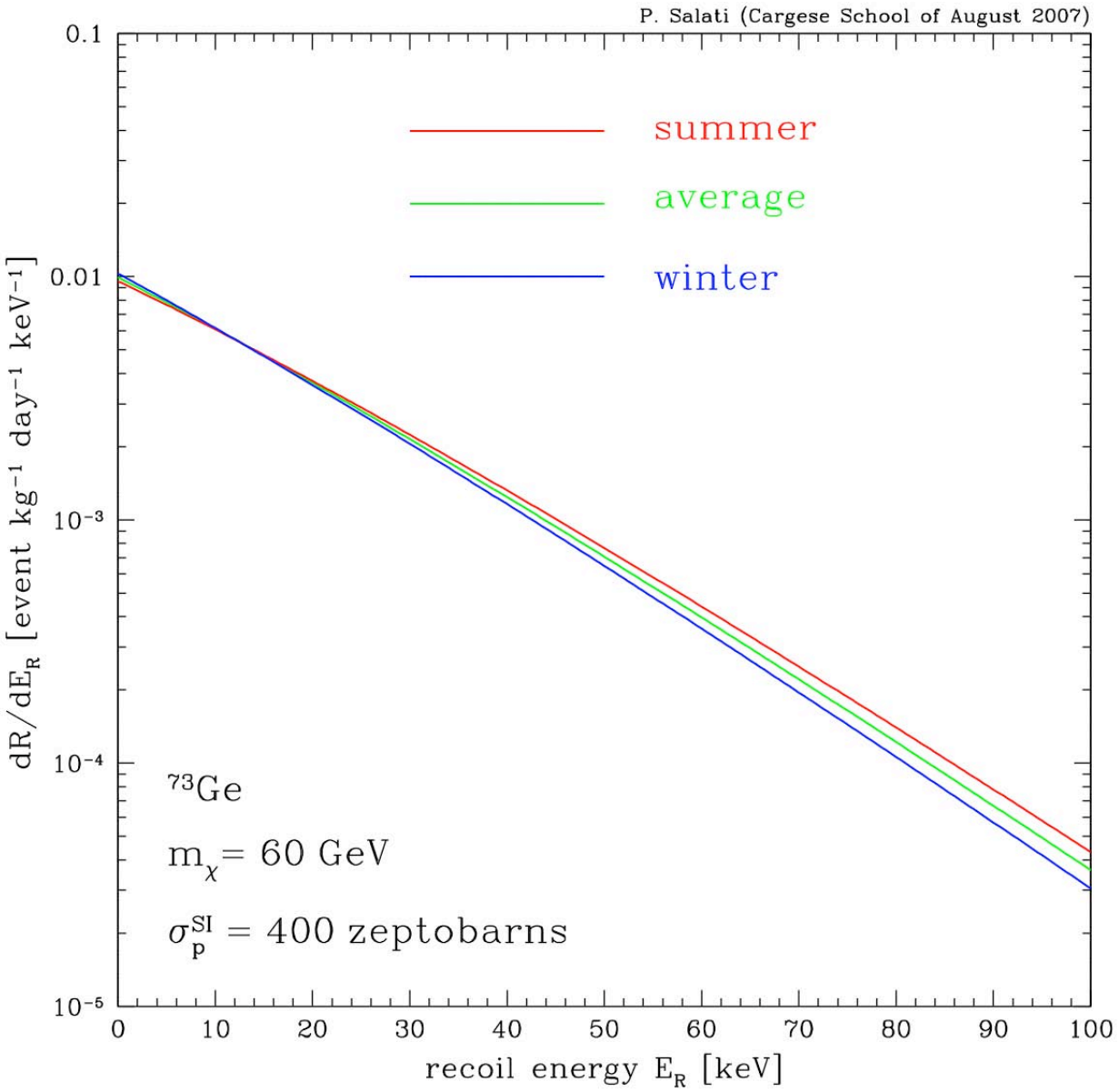
P. Salati (Cargese School of August 2007)
summer
average
winter
^{73}Ge
m_χ= 60 GeV
σ_p^{SI} = 400 zeptobarns
dR/dE$_R$ [event kg^{-1} day^{-1} keV^{-1}]
recoil energy E$_R$ [keV]
0.1
0.01
10^{-3}
10^{-4}
10^{-5}
0
10
20
30
40
50
60
70
80
90
100

DAMA/NaI

http://www.lngs.infn.it/site/meesem/DAMA/DAMA.pdf

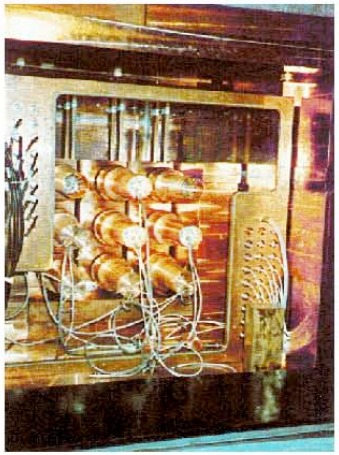

Gran Sasso Underground Laboratory (Italy)

- 100 kg NaI detector mass
- Scintillation +PSD
- Annual modulation
- Two targets: high (Na) and low mass (I)
- Sensitive to both spin-dependent and spin-independent interactions

7 years of data taking

Data taking completed on July 2002

Evidence of an annual modulation signature

A total exposure of : 107,800 kg-d

Rate has a component modulated with cosine function

Fit at 6.3σ C.L. : IJMPD13(2004)2127

A = (0.0200 ± 0.0032) cpd/kg/keV;
t0 = (140 ± 22) d ; T = (1.00 ± 0.01) y

$$m_\chi \sim 52 \text{ GeV}$$

$$\sigma_p^{SI} \sim 7.2 \times 10^{-6} \text{ pb}$$

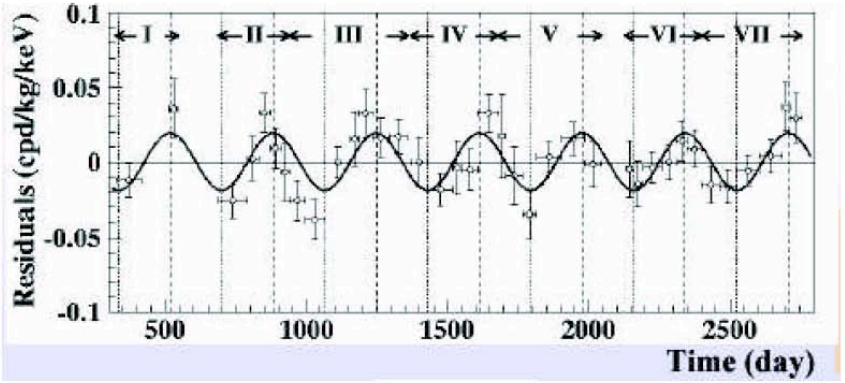

2-6 keV

Diurnal modulation ,Directionality :

Asymmetry on the direction of the recoiling nucleus because the wimp velocity distribution on the Earth is peaked in the opposite direction of the Earth motion in the galactic halo. The effect is much larger than the seasonal modulation : nigth-day asymmetry 7 - 17 %

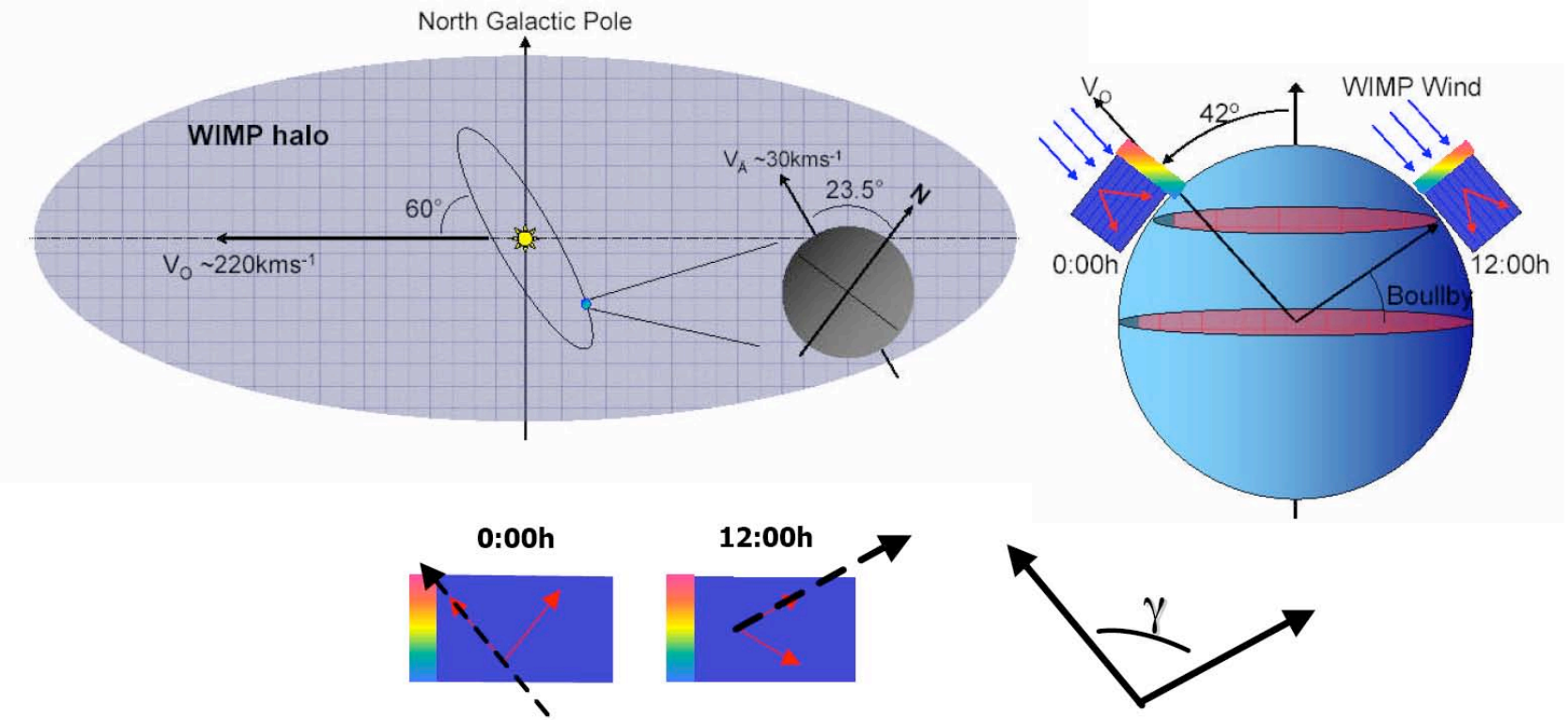

Neil Spooner
http://www.shef.ac.uk/physics/idm2002/talks/pdfs/spooner-summary.pdf

Directional Recoil Identification From Tracks

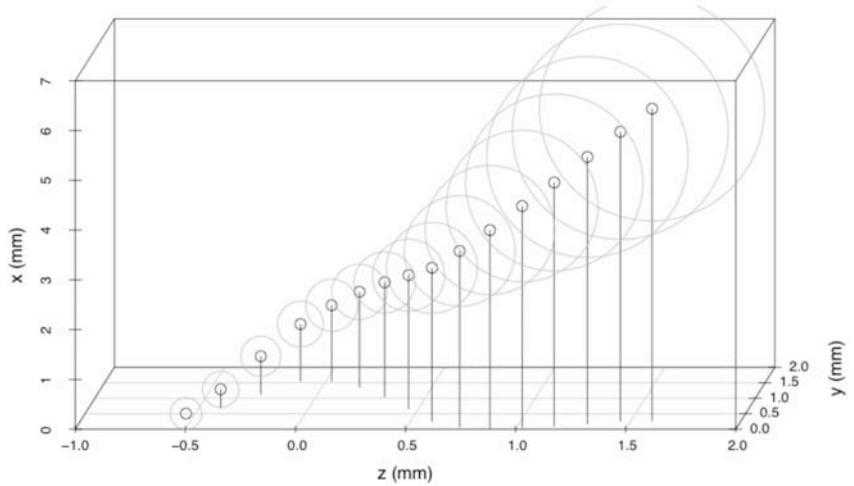

Figure 4: Example 3D reconstruction of a 100 keV S recoil track obtained with the DRIFT II directional dark matter detector. Circles are indicative of the energy deposited along the track.

[UKDMC]

Conclusions & Perspectives

- Direct DM search is a fast moving field with tremendous progresses in the past 20 years.
- Mildly subject to uncertainties – a factor of 10 – through $\rho_\odot$ and the WIMP velocity distribution.
- The zeptobarn goal is reacheable. Note that the top of the SUSY iceberg is already excluded.
- Complementarity between LHC and direct detection – for large neutralino masses especially.